AD-A041 087 GENERAL ELECTRIC CORPORATE RESEARCH AND DEVELOPMENT --ETC F/G 11/9
BISPHENOL FLUORENONE CARBONATE-SILICONE BLOCK POLYMERS: IMPROVE--ETC(U)
APR 77 R P KAMBOUR, J E CORN, H J KLOPFER N00019-76-C-0096

UNCLASSIFIED SRD-77-054 NL

1 OF 1
AD A041087

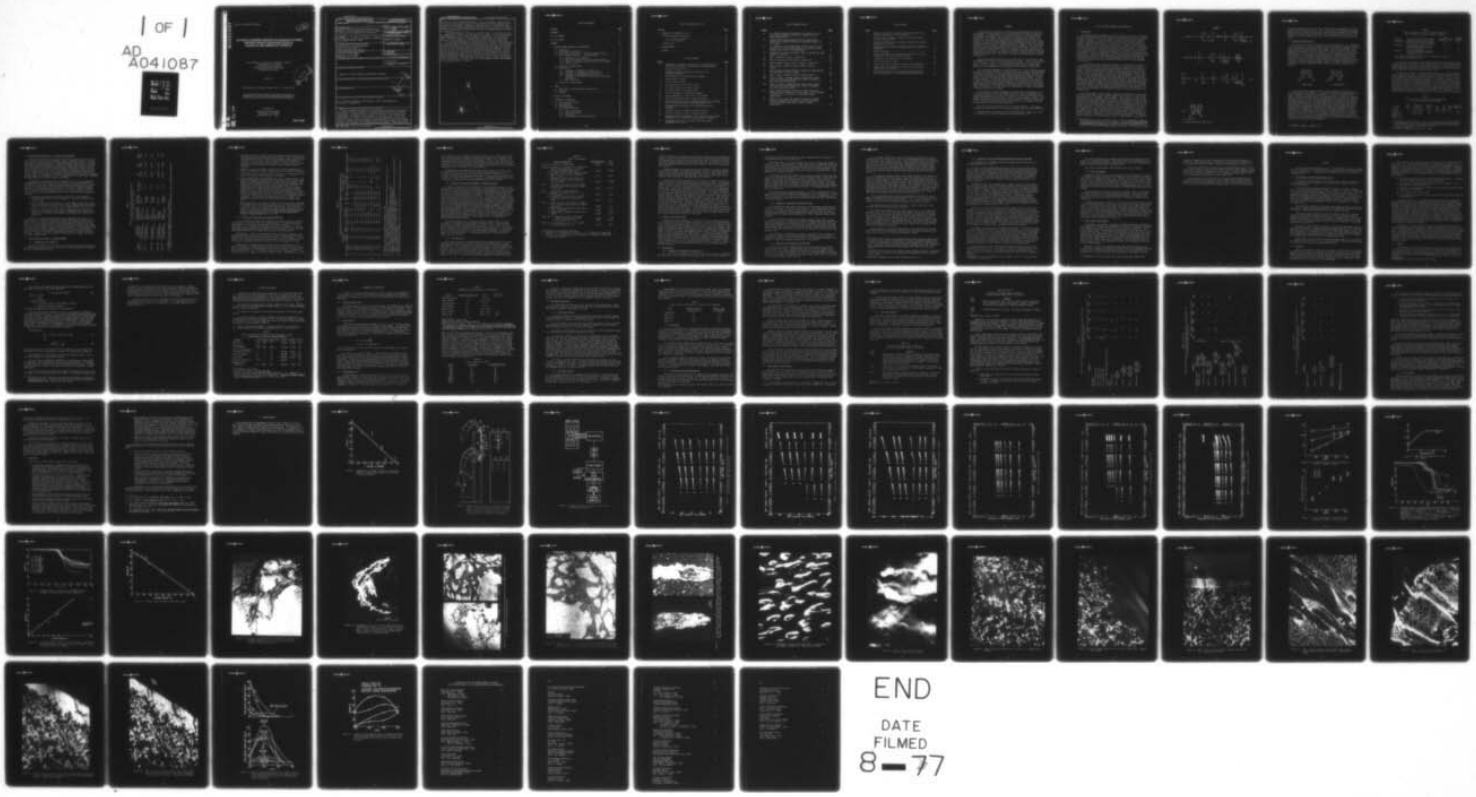

END

DATE FILMED
8-77

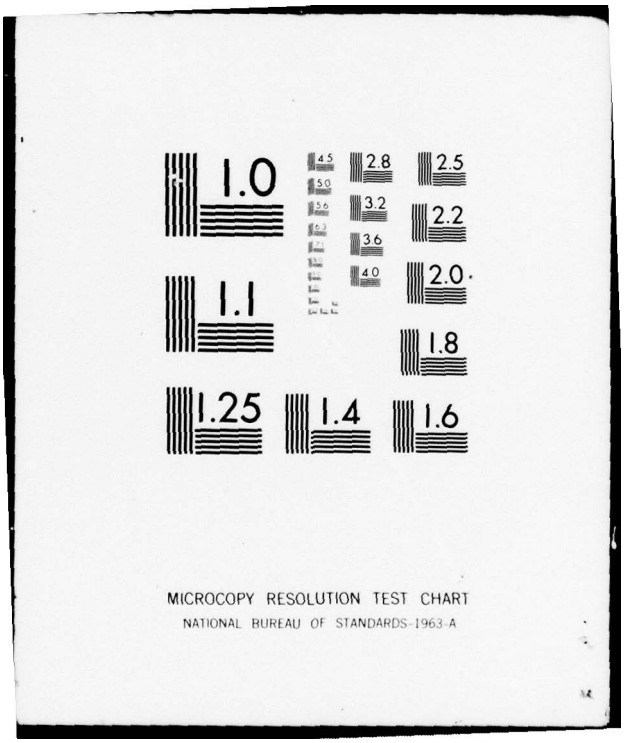
1.0
1.1
1.25
1.4
1.6
1.8
2.0
2.2
2.5
2.8
3.2
3.6
4.0
4.5
5.0
5.6
6.3
MICROCOPY RESOLUTION TEST CHART
NATIONAL BUREAU OF STANDARDS-1963-A

Contract No. N00019-76-C-0096

12

BISPHENOL FLUORENONE CARBONATE-SILICONE BLOCK POLYMERS: IMPROVED SYNTHESIS AND FURTHER STUDIES OF MECHANICAL AND FLAMMABILITY PROPERTIES

R.P. Kambour, J.E. Corn, H.J. Klopfer, S. Miller,
C.M. Orlando, and L.D. Stang
General Electric Company
Corporate Research and Development
Schenectady, New York

April 1977

Final Report for Period 22 October 1975 - 21 October 1976

Approved for public release; distribution unlimited.

Prepared for

Naval Air Systems Command
Department of the Navy
Washington, D.C. 20361

SRD-77-054

UNCLASSIFIED

SECURITY CLASSIFICATION OF THIS PAGE *(When Data Entered)*

REPORT DOCUMENTATION PAGE		READ INSTRUCTIONS BEFORE COMPLETING FORM
1. REPORT NUMBER	2. GOVT ACCESSION NO.	3. RECIPIENT'S CATALOG NUMBER
4. TITLE *(and Subtitle)* Bisphenol Fluorenone Carbonate-Silicone Block Polymers: Improved Synthesis and Further Studies of Mechanical and Flammability Properties.		5. TYPE OF REPORT & PERIOD COVERED Final Report. 22 Oct. 1975 - 21 Oct. 1976. 6. PERFORMING ORG. REPORT NUMBER SRD-77-054
7. AUTHOR(s) R.P. Kambour, J.E. Corn, H.J. Klopfer, S. Miller, C.M. Orlando, and L.D. Stang		8. CONTRACT OR GRANT NUMBER(s) N00019-76-C-0096
9. PERFORMING ORGANIZATION NAME AND ADDRESS Corporate Research and Development General Electric Company Schenectady, New York 12301		10. PROGRAM ELEMENT, PROJECT, TASK AREA & WORK UNIT NUMBERS
11. CONTROLLING OFFICE NAME AND ADDRESS Naval Air Systems Command Department of the Navy Washington, D.C. 20361		12. REPORT DATE April 1977 13. NUMBER OF PAGES 64
14. MONITORING AGENCY NAME & ADDRESS*(if different from Controlling Office)*		15. SECURITY CLASS. *(of this report)* Unclassified 15a. DECLASSIFICATION/DOWNGRADING SCHEDULE

16. DISTRIBUTION STATEMENT *(of this Report)*

Approved for public release; distribution unlimited.

17. DISTRIBUTION STATEMENT *(of the abstract entered in Block 20, if different from Report)*

406 617

18. SUPPLEMENTARY NOTES

19. KEY WORDS *(Continue on reverse side if necessary and identify by block number)*

block polymers, silicones, polycarbonate, tough, high temperature, transparent, flammability

20. ABSTRACT *(Continue on reverse side if necessary and identify by block number)*

Several changes in synthesis and processing procedures have resulted in BPF carbonate-silicone plastics of controlled molecular weight and improved transparency. Ultrapurification of the BPF monomer, use of rigorously dry environments and reagents, use of ammonia as the base in the silicone end-capping step, the return to chloroform as the polymerization solvent, the addition of excess base and phosgene during polymerization, and rapid polymer isolation washing and drying minimized molecular weight reduction and allowed effective use of phenol as a polymerization chain stopper. These steps also

DD FORM 1 JAN 73 1473 EDITION OF 1 NOV 65 IS OBSOLETE

UNCLASSIFIED

SECURITY CLASSIFICATION OF THIS PAGE *(When Data Entered)*

Continued from block 20.

resulted in almost complete elimination of haze in moldings. The purer BPF particularly and argon blanketing of the extruder led to much reduced color in extrudates and moldings. A number of synthesis personnel experienced skin rashes and eye irritation from working with BPF or in the vicinity of ongoing BPF work; biological tests tentatively confirmed the dermatological problems were encountered by personnel.

Creep studies were carried out on one resin over 5 to 6 decades of time at stresses up to 4200 psi and temperatures up to 80°C. Creep is proportional to $(\text{time})^n$ where $n \leq 0.03$. Little temperature dependence of creep rates is seen. Critical stresses for crazing under constant load are greater than 4000 psi at room temperature but approximately this level at 50 and 80°C.

The outstanding flammability characteristics of the BPF carbonate-silicone block polymer family have been confirmed with further testing. The mechanism previously proposed for the synergism between the BPF carbonate and the silicone blocks in raising the limiting oxygen index has been supported with the results of electron microscopy and controlled degradation studies. A layer of what appears to be vitreous SiO_2 has been found lining the outer pores of the char. Analyses of the volatile products and the residues of controlled degradation studies suggest that the BPF block prevents silicone cyclization until temperatures are reached where volatilized silicone reacts with ambient oxygen to form SiO_2. The SiO_2 layers are then thought to reduce the exposure of the underlying char to oxygen.

TABLE OF CONTENTS

Section		Page
ABSTRACT		i
LIST OF FIGURES		iv
LIST OF TABLES		vi
SUMMARY		vii
1.	BLOCK POLYMER SYNTHESIS AND PROCESSING	1
1.1	Background	1
1.2	BPF Monomer Purification	3
1.3	Block Polymer Synthesis -- Previous Contract Method	5
1.4	Block Polymer Synthesis -- Improved Method	5
1.4.1	Modification of Synthesis	5
1.4.2	Molecular Weight Control and Reproducibility	7
1.4.3	Effect of Isolation Procedure on Molecular Weight	9
1.4.4	Haze and Color	9
1.5	Summary of Synthetic Work	11
1.6	Experimental	11
1.6.1	Synthesis of Bisphenol Fluorenone (I)	11
1.6.2	Synthesis of Equilibrated Silicone Fluid	12
1.6.3	Synthesis of Endcapped Silicone Fluid	12
1.6.4	Synthesis of BPF Carbonate-Dimethylsiloxane Block Copolymer	14
1.6.5	Melt Processing	15
1.7	Toxicology of BPF Monomer	15
2.	CREEP	17
2.1	Multistation Constant-Stress Creep Tester	17
2.2	Procedure	17
2.3	Results	18
3.	CRAZING RESISTANCE	21
4.	FLAMMABILITY PROPERTIES	22
4.1	Limiting Oxygen Index	22
4.2	Smoke Density	22
4.3	Thermogravimetry	22
4.4	Char Characterization	24
4.4.1	Volume and Density	24
4.4.2	Char SiO_2 Content	24
4.4.3	Microscopy	25
4.4.4	Transmission Electron Microscopy	25

TABLE OF CONTENTS (Cont'd)

Section		Page
4.	FLAMMABILITY PROPERTIES (Cont'd)	
	4.5 High-Temperature Chemistry	26
	4.5.1 Volatile Products	27
	4.5.2 Gel Formation	32
	4.6 Discussion	33
5.	ACKNOWLEDGMENTS	35
	FIGURES	36

LIST OF FIGURES

Figure		Page
1	Dependence of intrinsic viscosity [η] of resin powder on chain stopper (phenol) concentration in reaction mixture	36
2	Six-station creep tester	37
3	Schematic diagram of creep data acquisition and processing equipment	38
4	Creep behavior at 28°C and several stresses	39
5	Creep behavior at 50°C	40
6	Creep behavior at 80°C	41
7	Log creep strain vs log time at 28°C	42
8	Log creep strain vs log time at 50°C	43
9	Log creep strain vs log time at 80°C	44
10	Stress dependence of creep time exponent n	45
11	Stress dependence of creep rate at 10^3 seconds	45
12	ASTM limiting oxygen index vs silicone content	46
13	Thermogravimetric analyses of BPF polycarbonate in nitrogen and of silicone gum and all BPFC/DMS resins in air	46
14	Thermogravimetric analyses of all BPF/DMS resins in nitrogen	47
15	TGA (air) residue at 700°C vs silicone content	47
16	TGA (N_2) residue at 700°C vs silicone content	48
17	Scanning electron micrograph of LOI char from block polymer 10053-136C (21.5 % silicone) before mounting in epoxy	49
18	Petrographic section of LOI char 10053-136C vacuum-impregnated with epoxy	50

LIST OF FIGURES (Cont'd)

Figure		Page
19	a) Scanning electron micrograph of an external part of char shown in Figure 17 and 18; b) portion of a) at higher magnification	51
20	Scanning electron micrograph formed by using excited silicon X-ray emission intensity to modulate cathode ray tube image	52
21	a) Specimen of resin 10053-136C, partially burnt at 50 % oxygen, prior to epoxy impregnation; b) section of same specimen after epoxy vacuum impregnation	53
22	Transmission electron micrograph (TEM) of ultrasection from region 1, Figure 21b	54
23	TEM of globule in region 1, Figure 21b	55
24	TEM of ultrasection from region 2, Figure 21b.	56
25	TEM of external edge of char in region 3, Figure 21b	57
26	TEM of region 3 showing internal channel with wall lining	58
27	TEM of region 3 showing internal channel with subdivisions of same material as wall lining.	59
28	TEM of region 3 showing fractured lining material.	60
29a	TEM's of region 3 showing channel lining (upper right) before electron beam intensity was raised to maximum to burn away resinous materials	61
29b	TEM's of region 3 showing channel lining (upper right) after electron beam intensity was raised to maximum to burn away resinous materials	62
30	Major volatile products collected in Tenax tubes from thermo-oxidative degradation of one sample of block polymer 10053-132C (24 % silicone) at successively higher temperatures	63
31	Weight loss and insoluble fraction produced by thermo-oxidative degradation of samples of BPF polycarbonate and block polymer 10053-132C at each of several temperatures	64

LIST OF TABLES

Table		Page
1	Effect of Isolation and Purification Procedure on Color and BPF (II) Content of BPF (I) Monomer.	4
2	Effect of BPF (I) Purity on Molecular Weight and Color of Block Polymer Powder.	4
3	Results from Modification of Polymer Synthesis to Enhance Homogeneity of System.	6
4	Analytical Data on Block Copolymers Prepared Via Modified Synthesis.	8
5	Haze in Moldings	10
6	Critical Stresses (σ_c) and Critical Strains (ε_c) at Room Temperature for Several Glassy Polymers.	21
7	Flammability Characteristics of BPF Resins	23
8	TGA (N_2) Residues at 700°C	23
9	Weight Loss from LOI Chars as a Result of HF Digestion . . .	25
10	Observations During Stages of Heating of Block Polymer 10053-132C in Air Stream	27
11	Major Volatile Products from Thermooxidation of Block Polymer 10053-132C at Successively Higher Temperatures . . .	29

SUMMARY

Several changes in synthesis and processing procedures have resulted in BPF carbonate-silicone plastics of controlled molecular weight and improved transparency. Ultrapurification of the BPF monomer, use of rigorously dry environments and reagents, use of ammonia as the base in the silicone end-capping step, the return to chloroform as the polymerization solvent, the addition of excess base and phosgene during polymerization, and rapid polymer isolation washing and drying minimized molecular weight reduction and allowed effective use of phenol as a polymerization chain stopper. These steps also resulted in almost complete elimination of haze in moldings. The purer BPF particularly and argon blanketing of the extruder led to much reduced color in extrudates and moldings. A number of synthesis personnel experienced skin rashes and eye irritation from working with BPF or in the vicinity of ongoing BPF work; biological tests tentatively confirmed the dermatological problems encountered.

Creep studies were carried out on one resin over 5 to 6 decades of time at stresses up to 4200 psi and temperatures up to 80°C. Creep is proportional to time ^{n} where $n \leq 0.03$. Little temperature dependence of creep rates is seen. Critical stresses for crazing under constant load are greater than 4000 psi at room temperature but approximately this level at 50 and 80°C.

The outstanding flammability characteristics of the BPF carbonate-silicone block polymer family have been confirmed with further testing. The mechanism previously proposed for the synergism between the BPF carbonate and the silicone blocks in raising the limiting oxygen index has been supported with the results of electron microscopy and controlled degradation studies. A layer of what appears to be vitreous SiO_2 has been found lining the outer pores of the char. Analyses of the volatile products and the residues of controlled degradation studies suggest that the BPF block prevents silicone cyclization until temperatures are reached where volatilized silicone reacts with ambient oxygen to form SiO_2. The SiO_2 layers are then thought to reduce the exposure of the underlying char to oxygen.

The production in larger quantities of resins that are uniformly low in color level and haze is the most important task of future development work. To ensure reproducibility of low color levels the factors governing BPF color levels need further definition (e.g., effect of light, oxygen, solvents, etc.). Further refinement of the extrusion process should be undertaken, since much of the color in extrudates develops at this point (e.g., extrudate surfaces are more highly colored than are interiors).

Haze and optical distortion need to be further reduced. For further advances here the character of the light scattering bodies may need definition.

Among the physical properties still uncharacterized, resistance to solvent crazing and to abrasion probably deserve definition first.

1. BLOCK POLYMER SYNTHESIS AND PROCESSING

1.1 Background

The dimethylsiloxane bisphenol fluorenone carbonate block polymer synthesis has been systematically investigated on both small and large scale over a period of four years. The basic synthetic process which has been developed is shown in Scheme I and was described in detail in the previous contract report.[1] Various modifications of this basic process have been employed to simplify handling, particularly on a large scale. However, without respect to scale, the nature of the chemistry involved in this synthesis is such that the resulting polymers possess a high degree of polydispersity.[1] The nature of the polydispersity is affected by the reaction variables in each step of the synthesis as well as competing formation of cyclic BPF carbonates during phosgenation. Together, these make it difficult to prepare reproducibly these block polymers with given molecular weight, composition, and distribution. Throughout the history of this contract research, a problem which was regularly encountered was the lack of molecular weight control in the phosgenation reaction.

At the conclusion of the previous contract, the small-scale syntheses of block polymers (13 to 19% silicone) were shown to provide resins of more closely controlled silicone content and molecular weight than previously observed. Numerous factors such as reagent purity, pH control, and reactant addition rate were identified as critical in maintaining this control. However, a study of chain stopper efficiency in the phosgenation reaction indicated that the polymerizations are self-limiting with respect to molecular weight. On the basis of the data from these small-scale syntheses, the block polymers were successfully scaled up in three stages to the three pound level. Even though molecular weight was self-limiting, several polymerizations gave reproducible molecular weights that were sufficiently high for the processed materials to display uniformly good strength properties. The block polymers (13 to 24% silicone) were processed by extrusion and injection molding. In many cases the extrudates and moldings were dark yellow to straw-colored and slightly hazy.

Color development in the processed resin was considered to be associated with BPF monomer purity and/or thermal instability of the block polymer system resulting from incomplete chain stopping. The appearance of haze in the processed resin was considered to be related to phase separation due to excessive spread in composition and/or block length distributions. Based upon the results of the previous contract research, it was concluded that the most important task to be undertaken in the next stage of development of this block polymer system was to reduce color and haze in the processed block polymer. To accomplish this goal, exhaustive purification of BPF monomer from a scale-up synthesis was planned in an attempt to reduce monomer color and remove impurities, which could function as chain stoppers in the polymerization reaction as well as contribute to color in the processed polymer. In addition, improved conditions for polymerization would be investigated to gain control

1. R.P. Kambour, J.E. Corn, S. Miller, and G.E. Niznik, Bisphenol Fluorenone Carbonate-Dimethylsiloxane Block Polymers: Transparent, Tough, Heat- and Flame-Resistant Thermoplastics, Final Report, Contract Number N00019-74-C-0174 for the Naval Air Systems Command, Department of the Navy, July 1975.

Scheme I

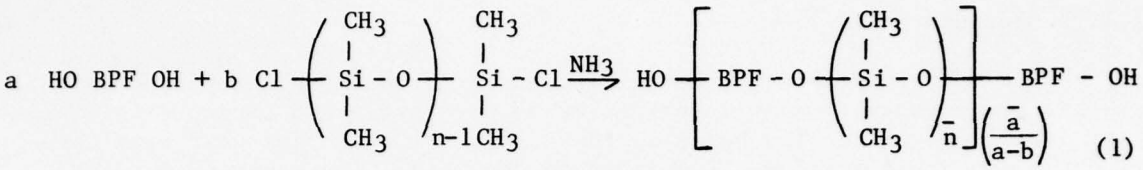

(1)

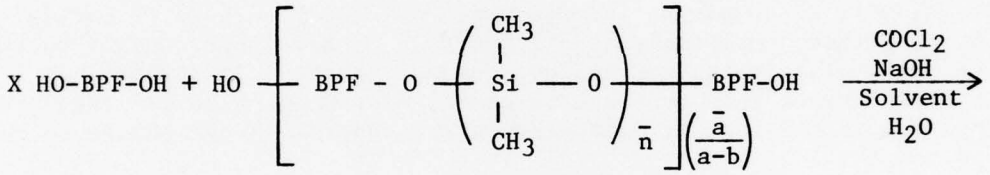

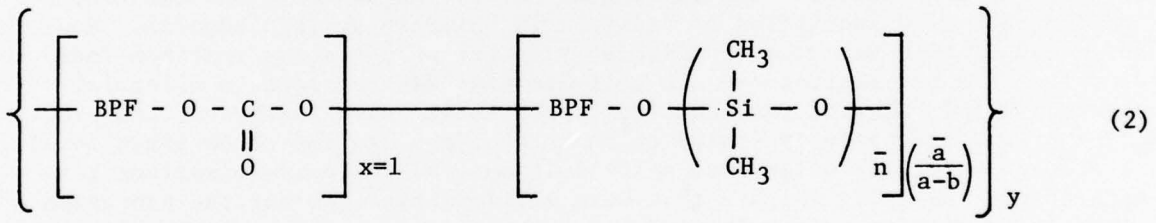

(2)

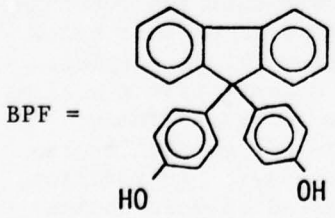

a = moles BPF

b = moles dichlorosilicone fluid

of molecular weight in this reaction, a factor which was considered to effect haze in processed block polymer. Lastly, several three-pound batches of block polymer would be prepared incorporating the necessary improvements considered important in color and haze reduction. This material would also serve to complete the profile of engineering properties on extruded and injection-molded resin.

1.2 BPF Monomer Purification

As previously discussed, impurities in the BPF monomer (I) are considered a potential cause of color development in the processed block polymer, in addition to limiting the polymer molecular weight. The color development could result from the residual monomer color which is carried over into the corresponding polymer and/or the incorporation of a known impurity (the o,p-isomer of BPF (II)) into the polymer as a chain stopper. Although this isomer is bifunctional, the orthohydroxyl group may be sufficiently hindered to lower its reactivity substantially in the polymerization reaction; thus (II) may function in effect as a chain stopper, limiting molecular weight and resulting in phenolic hydroxy-terminated polymer chains. The thermal instability of this type of polymer end group in polycarbonates has been previously established.[2]

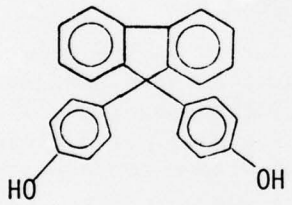

I, BPF (p,p)

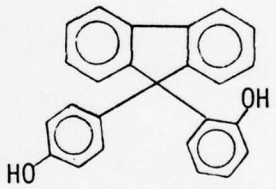

II, BPF (o,p)

The standard BPF synthesis involves the HCl-catalyzed condensation of 9-fluorenone with excess phenol. The previous isolation and purification procedure employed an azeotropic distillation of the water of reaction with decane, followed by distillation of the excess phenol, and finally a crystallization of the crude BPF (I) from nitromethane. This procedure yielded BPF (I) containing 0.5% or less of the isomeric BPF (II), which was then used for subsequent polymerization. The improved procedure developed in the current work involves isolation of the crude monomer by crystallization from the reaction mixture, using methanol/H_2O (1.1/1 volume), and subsequent recrystallization from nitromethane. This procedure provides the monomer with ca. 0.1% BPF II. A comparison of the color of the monomer made by the old and new procedures for isolation and purification is shown in Table 1. Note the significant decrease in color in the monomer obtained by the new procedure (entry 2 vs 1). The color of the monomer via the new procedure (entry 2) is even lower than the monomer obtained by the old procedure which has been twice treated with activated charcoal (entry 3).

2. A. Factor, private communication.

TABLE 1

Effect of Isolation and Purification Procedure on
Color and BPF (II) Content of BPF (I) Monomer

BPF (I)	Isolation and Purification Procedure	Color Number $\times 10^3$[a] (1/g)	Percent BPF (II)
1. 10053-82AX1	Azeotropic distillation with decane. One crystallization from nitromethane.	16.0	5
2. 22976 BPF	Methanol/H_2O crystallization from reaction mixture. Recrystallized once from nitromethane.	2.2	5
3. 10330-22	Above BPF (10053-82AX1), dissolved in methanol and treated twice with activated charcoal.	3.2	0.1

a - Color number = absorbance at 400 nm per unit concentration, using 10 cm path length spectrophotometer cell.

The use of nitromethane as a purification solvent has been effective in lowering the BPF (II) content of the crude monomer to ~0.1% only if the crude monomer contains less than 5% of the isomeric impurity. Crude monomer with isomer impurity levels greater than 5% can be more effectively purified with acetonitrile used as the recrystallization solvent.

To evaluate the effect of improved BPF (I) purity on the color and molecular weight of the polymer, identical polymerizations were performed with the two grades of monomer as described in Table 1 (entries 1 and 2). Polymer powders were obtained, evaluated, and found to have distinct differences in color and intrinsic viscosities (see Table 2). A direct correlation between monomer color and the corresponding polymer color was observed. As a reference point for the color of block polymer, an entry for Lexan® polycarbonate polymer is included. Based on the intrinsic viscosity data shown in Table 2, it is apparent that the concentration of the isomer impurity BPF (II) in the monomer is much too low to explain the low observed [η]. Therefore, some other factor is involved in the limitation of molecular weight in this system.

TABLE 2

Effect of BPF (I) Purity on Molecular Weight
and Color of Block Polymer Powder

Polymer	BPF[a] Source	Polymerization Method	[η] $CHCl_3$ (dl/g) 25°C	$\bar{M}w$[c]	$\bar{M}n$[c]	$\bar{M}w/\bar{M}n$	Color Number[d] $\times 10^3$
10563-63	A	Aqueous caustic[b]	0.53	83,600	12,200	6.82	6.0
10563-96A	B	Aqueous caustic[b]	0.83	155,100	19,800	7.84	2.3
Lexan® BPA polycarbonate powder (natural grade)	--	Aqueous caustic	0.48	--	--	--	1.04

a - A = BPF purified by method in entry 1, Table 1; B = BPF purified by method in entry 2, Table 1.
b - Phosgenation reaction done by aqueous caustic method (see subsection 1.6, "Experimental").
c - Apparent molecular weights by gel permeation chromatography using a polystyrene calibration. See Ref. 1 for relationship between apparent and real Mn's.
d - See Table 1 for definition.
® - Registered trademark of the General Electric Company.

1.3 Block Polymer Synthesis -- Previous Contract Method

Employing the monomer that was made under the previous contract and partly used at that time in scale-up syntheses, several attempts were made to repeat that work on a three-pound scale. These attempts were unsuccessful. The polymers which were isolated were low in molecular weight ($[\eta] \simeq 0.2$) and unstable for further thermal processing and evaluation. When purified BPF (I) (procedure 2 in Table 1) was used in the block polymer synthesis, a higher molecular weight polymer was obtained ($[\eta] \simeq 0.55$); however, degradation occurred on injection molding ($[\eta] \simeq 0.3$). The moldings were badly splayed and delaminated easily. After the unexpected difficulty in reproducing the previously successful polymer synthesis, investigation of the polymerization on a small scale (28-280 g) was undertaken in an attempt to solve the problem.

On the basis of past experience, heterogeneity in both the endcapping of the equilibrated silicone fluid and the aqueous caustic polymerization were considered to affect both average molecular weight and molecular weight distribution. The latter factor greatly influences structural integrity, physical properties, and transparency of the polymer. In order to enhance the homogeneity in these two steps and determine its effect on the properties of the final polymer, the following modifications in the synthesis were independently examined:

- Endcapping the equilibrated silicone fluid with a stoichiometric quantity of BPA (a more soluble bisphenol), followed by copolymerization with BPF.
- Use of solvents other than CH_2Cl_2 to try to enhance solubility of BPF and its sodium salts (solvents used: $CHCl_3$, $CHCl_3/CH_2Cl_2$, $CHCl_3/CH_2Cl_2$/dioxane). This work was done using the BPA-endcapped silicone fluid.
- Use of the anhydrous pyridine method of phosgenation polymerization instead of the aqueous caustic method. Endcapped fluid, monomer, and polymer are all soluble in pyridine, and the reaction is thus a homogeneous one.

The results of these investigations can be summarized by stating that while moderate to high molecular weight polymers were obtained, there was very little control of intrinsic viscosity and molecular weight distribution (see Table 3). All the polymers made in this study resulted in solvent cast films that varied from slightly cloudy to opaque. Previous experience has shown that cloudy cast films forecast cloudy melt processed polymer. It was apparent from this work that increased homogeneity in the critical steps of the synthesis provided polymer of sufficiently high molecular weight to possess structural integrity. Further steps were required to bring molecular weight characteristics under tight control.

1.4 Block Polymer Synthesis -- Improved Method

1.4.1 Modification of Synthesis

The chronic difficulties with control of molecular weight characteristics were finally eliminated by use of the previously outlined synthetic procedure[1] with the following modifications:

TABLE 3

Results from Modification of Polymer Synthesis
to Enhance Homogeneity of System

Polymer	Synthesis Modification	Polymerization Method/Solvent	Clarity of Cast Film	[η] (dl/g)[a]	Mw[b]	Mn[b]	Mw/Mn
10563-72B	BPA endcapped fluid/BPF monomer	Aqueous caustic/$CHCl_3$	Opaque	1.08	251,900	30,800	8.18
10563-76	BPA endcapped fluid/BPF monomer	Aqueous caustic/$CHCl_3$ CH_2Cl_2	Slightly cloudy	0.43	56,160	18,120	3.10
10563-78A	BPA endcapped fluid/BPF monomer	Aqueous caustic/$CHCl_3$ CH_2Cl_2	Slightly cloudy	0.97	194,718	16,971	11.47
10563-80A	BPF endcapped fluid/BPF monomer	Pyridine/ $ClCH_2CH_2Cl$	Cloudy	0.79	163,990	46,211	3.55
10563-68B	BPF endcapped fluid/BPF monomer	Aqueous caustic/$CHCl_3$	Slightly cloudy	0.75	129,530	32,820	3.95

a - Intrinsic viscosity measured at 25°C in chloroform.
b - Apparent molecular weights by gel permeation chromatography, using a polystyrene calibration.

a. Rigorously anhydrous conditions were maintained in the preparation of equilibrated and endcapped equilibrated silicone fluids. All glassware was flame-dried and all transfers and weighings of the reagents were carried out in a dry box. This procedure reduces the tendency of chlorosilane groups to hydrolyze to silanols. (The latter react with phosgene to form hydrolytically unstable silanol-phenol carbonate linkages.)

b. Ammonia was used as the base in the silicone fluid endcapping step. Unlike triethylamine, ammonia renders the reaction mixture homogeneous.

c. Chloroform was used instead of dichloroethane as the phosgenation solvent. The polymer is more soluble in the former.

d. Excess aqueous caustic and phosgene were used in polymerization. The previous phosgenation procedure was conducted at pH 9.5, using approximately stoichiometric quantities of aqueous NaOH and phosgene. The side reaction of phosgene and base to yield CO_2, NaCl, and water may, depending on conditions, be fast enough compared with the rate of polymerization to consume significant amounts of base and phosgene. These reagents were thus metered into the reaction mixture simultaneously at rates by which pH 11 was maintained throughout the reaction. Reagent stoichiometry was ignored. Instead, base and phosgene addition were continued until the viscosity of the reaction mixture stopped increasing. In some block copolymer syntheses, up to 300% of the theoretical amounts of aqueous sodium hydroxide and phosgene were used.

e. The polymerization and isolation stages of the block polymer synthesis were conducted in one continuous operation to the final dried material, to minimize polymer molecular weight degradation. In the previous contract procedure, the synthetic sequence was interrupted at various stages for convenience. At the time, these stages were considered to present conditions under which the polymer was not susceptible to molecular weight degradation. (cf 1.4.3)

1.4.2 Molecular Weight Control and Reproducibility

A block copolymer synthesis was conducted utilizing the general procedure described in the previous report and incorporating all the modifications described above. The polymer obtained had an intrinsic viscosity of 3.0 dl/g., the highest of any BPFC/DMS block polymer made to date. Moreover, it was evident that further increases were limited only by an inability to stir the mixture properly because of the high viscosity of the reaction mixture.

Subsequently, a series of polymerizations was conducted according to the modified procedure, using identical starting materials (BPF monomer, BPF endcapped fluid, solvents) and varying levels of phenol as chain stopper. (Resins of $[\eta] > 1.0$ dl/g have excessive melt viscosities.) The data obtained from this study are presented in Table 4 (entries 1-5) and in Figure 1 (p. 36).

Theoretically, polymer molecular weight should be proportional to the molar concentration of bifunctional units (BPF plus endcapped silicone) divided by the concentration of chain stopper in the reaction mixture. Further, $[\eta] = kM^{\alpha}$ usually where $\alpha \simeq 0.7$. Thus theoretically $\log [\eta] \propto \log [\text{phenol}]^{-0.7}$. The slope of the line in Figure 1 is -0.46. However, within experimental error the

TABLE 4

Analytical Data on Block Copolymers Prepared Via Modified Synthesis

Run	Polymer	Theoretical Yield Polymer[g]	Mole % Phenol	% Yield	[η](dl/g)[a] Powder	[η](dl/g)[a] Film	GPC $\bar{M}w$	GPC $\bar{M}n$	GPC $\bar{M}w/\bar{M}n$	Color Number × 10^{3}[b] Powder	Color Number × 10^{3}[b] Extrudate Air	Color Number × 10^{3}[b] Extrudate Argon	Fe(ppm)[c]	% Silicone[d]
1	9676	28	0	90.4	2.91	3.16	e	e	e	4.9[h]	g	g	5.6	25.3
2	92176	28	0.065	90.7	2.65	2.41	e	e	e	3.3[h]	g	g	4.4	24.0
3	92376	28	0.26	75.6	2.20	1.71	68.73	308.5	2.23	3.0[h]	-	-	3.6	26.6
4	92976	28	0.52	78.9	1.34	1.28	370.3	55.6	6.66	2.2[h]	g	g	30.1	26.6
5	93076	28	1.04	79.2	0.89	0.85	141.9	20.0	7.09	1.8	g	g	15.2	24.8
6	10476	28	1.30	78.2	0.90	0.84	150.4	30.7	4.89	1.7	g	g	5.0	25.3
7	10676	28	1.3	76.8	0.88	--	174.7	42.3	4.14	2.2	g	g	1.5	24.0
8	10776	140	1.30	83.2	0.48[f]	--	62.2	23.4	2.66	1.8	7	-	5/13.7	24.5
9	112476	1372	1.6	92.8	0.46	0.54	77.8	22.9	3.39	10.6	200	64	7.1/8.2	24.5
10	1577	140	1.3	81.6	0.60	--	106.3	28.0	3.80	-	-	54	10.5/11.5	
11	12577	280	1.3	68.2	0.61	--	101.4	21.7	4.67	3.3	-	105	2.1	27.7
12	2277	190	1.3	76.3	0.62	0.70	129.8	41.7	3.11	1.3	-	10	2.6	25.8

a - Intrinsic viscosity measured in chloroform at 25°C.
b - Color number = absorbance of 2.5 g polymer in 50 m/chloroform at 400 nm/concentration in g/1.
c - Iron content in powder/iron content in extrudate.
d - Percent silicone tabulated experimentally measured (design value is 30%).
e - Molecular weight of this sample too high to obtain accurate GPC data.
f - Sample of this polymer when dried had [η] (dl/g) = 0.85. Mechanical problem with oven during drying of bulk of the polymer resulted in molecular weight reduction.
g - Polymer powders not extruded.
h - Solution filtered under pressure because of high viscosity. Not as efficient as gravity filtration.

data in Figure 1 can be fitted by a line of slope = -0.7. These results show that in the synthesis procedure as modified here phenol chain stopping occurs at a rate proportional to phenol concentration. Whether it is completely incorporated by the end of the reaction is unknown. In any case, phenol provides an effective and practical means of controlling molecular weight and reducing the hydroxy aryl end groups, which are thought to be unstable at melt processing temperatures and to contribute to color formation.

Although molecular weight control was achieved on the 28 g scale, as described above, some difficulty was encountered in reproducing the log [η] - log [phenol] relationship on a larger scale (cf Table 4, entries 10, 11, 12 vs 6 and 8). Further investigation of this effect of scale on the intrinsic viscosity/chain stopper relationship is necessary to determine whether this effect is chemical or mechanical (e.g. stirring efficiency) in its origin.

1.4.3 Effect of Isolation Procedure on Molecular Weight

It has been found that the interruption of the isolation sequence at any point from the polymerization stage through to the powder drying stage is likely to result in significant polymer molecular weight degradation. A block copolymer reaction solution prepared by the aqueous caustic phosgenation method was neutralized by successive washing and sampled. The polymer isolated from the sample had an intrinsic viscosity of 0.83 dl/g. The bulk of the polymer solution was allowed to stand for three days, and a polymer sample isolated at this point had an intrinsic viscosity of 0.44 dl/g. Subsequent precipitation of the bulk of the polymer and drying showed no change in measured intrinsic viscosity. Separate experiments demonstrated that polymer allowed to stand in the precipitation solvent (CH_3OH/acetone) for 40 hours underwent degradation, the intrinsic viscosity dropping from 1.07 to 0.58 dl/g. Based upon these results, each subsequent preparation of block polymer was performed in a continuous operation from polymerization to isolated polymer prior to oven drying. In order to avoid molecular weight reduction during drying it was found necessary to evacuate the powder at room temperature for several hours, to remove most of the remaining precipitation solvent. Only at that point could temperature be safely raised for final drying.

The effectiveness of the continuous operation during isolation on the maintenance of polymer molecular weight is shown in Table 4 under intrinsic viscosities of polymer film and powder (cf entries 1 to 6). The film represents a sample of the polymerization mixture taken before the bulk of the polymer is precipitated; the powder is the final isolated material. A comparison of the intrinsic viscosities of the film and powder represents the molecular weight loss during isolation. In these polymerizations, minimal molecular weight loss was observed.

1.4.4 Haze and Color

The haze or cloudiness observed previously in varying degrees in cast or compression-molded films, in polymer films cast from solution, and in extrudates has been almost eliminated in polymers made by the improved synthesis (see Table 5). This synthesis has resulted in polymers with reproducibly high molecular weights and moderately narrow distributions. Indeed, there is a rough correlation between the turbidity levels of the best moldings of the block polymers in Table 5 and the narrowness of their molecular weight distributions. The best of the moldings [112476(1)] exhibits a turbidity only 35%

TABLE 5

Haze[a] in Moldings

Resin and Specimen	Thickness (in.)	τ[b]
Lexan® polycarbonate extruded sheet	0.125	0.394
112476(1) Extrudate, flood feed, T's = 335-340°C, argon, 40 rpm, molded once at 310°C, 2nd time at 290°C; under argon	0.148	0.534
(2) Extruded at 305 to 335°C, argon, 80 rpm, molded at 310°C and then remolded at 290°C - argon	0.117	0.574
(3) Extrudate, starve to flood feed, T's 335-340°C, argon, 40 rpm, molded two times at 290°C.	0.128	0.669
12577 Extrudate, flood feed, T's 325-335°C, 100 rpm, argon; twice molded at ∿300°C under argon	0.122	0.772
12577 (redissolved, reprecipitated)		
(1) Extrudate, variable feed, T's 325 to 340°C, argon;	0.127	1.06
(2) Extrudate, flood feed, all T's 325°C, argon twice molded at ∿300°C under argon	0.130	1.15
2277 (1) Argon extrusion, flood feed, T's 330 to 335°C, 110 rpm, twice molded at ∿300°C under argon	0.129	1.12
(2) Same extrusion and molding conditions as (1) except 80 rpm	0.094	2.42
(3) Virgin powder compression molded once at ∿300°C	0.089	0.553
10053-132c (1) Extruded in 1975 in air, twice molded under argon at ∿300°C	0.121	2.25
(2) Same conditions as (1)	0.129	4.23
10053-136c Air extrusion; 2 in. × 2 in. plaque injection molded in 1975	0.121	2.27

a - As measured with Gardner haze meter.

b - Turbidity, τ, as defined by $I_s/(I_s+I_{tr}) = 1-e^{-\tau/d}$ where I_s = integrated intensity of scattered light, I_{tr} = intensity of transmitted light, and d is specimen thickness.

greater than that of a randomly selected piece of commercial polycarbonate extrudate. While there are several factors which affect the optical properties of polymers, many of the hazy block polymers that have been made in the past had low molecular weights and/or broad distributions. As a result of the current work, improved control of the optical clarity of the block polymers has been achieved.

Molded specimens low in haze, ground and polished to an optical finish, show an optical defect not previously noticed. A subtle, fine-grain optical distortion can often be seen when the molding is held at arm's length and a distant scene viewed through the specimen. The cause of this effect is not known but may be related to rheology and/or birefringence.

As previously noted (see subsection 1.1) there is a direct correlation between the color of the monomer and its corresponding polymer. The polymers listed in Table 4 have all been prepared from highly purified BPF monomer (see Table 1, entry 2) and have very low measured color levels. The polymer obtained from a large-scale polymerization (Table 4, entry 9) has a much higher color number, which is attributed to color development in the polymerization as a result of a substantially longer reaction time. The thermal processing of the block copolymers by extrusion always results in an increase in color to varying degrees. There is some evidence that extrusion under argon results in lower color than extrusion done under air (Table 4, entry 9). Iron analyses on both powders and extrudates were obtained to determine the effect of iron content on extrudate color. There is no apparent correlation of color with iron content in these block copolymers. Two polymers (Table 4, entries 7 and 12) prepared in this series have the lowest color numbers observed to date. Additional studies are required for an understanding of the reason for the observed variation in extrudate color. It is also noteworthy that color and haze levels are not generally correlated, although the last resin made (2277) gave the lowest color level of all while a bar molded from its powder directly exhibited the second lowest haze level (Table 5).

1.5 Summary of Synthetic Work

Confronted with the inability to reproduce the block copolymer synthesis on a large scale as done in the previous contract, several basic modifications in the synthetic process were made. Ultrapurification of the monomer and alteration of the polymerization conditions were the most significant changes. The modified polymerization procedure was found to be no longer self-limiting with respect to molecular weight. A systematic study of chain stopper concentration versus intrinsic viscosity established molecular weight control and reproducibility in the polymerization on a small scale. A continuous operation from polymerization to polymer isolation provided a method for maintaining polymer molecular weight during isolation. The block copolymers prepared under these conditions were optically clear as films and extruded rods. Polymer powder color intensities were low, but these increased on thermal processing. Several polymers made in this series maintained very low color from powder through thermal processing.

1.6 Experimental

1.6.1 Synthesis of Bisphenol Fluorenone (I)

Into a 12-liter round-bottom flask fitted with paddle stirrer, thermometer, gas inlet tube, reflux condenser, and nitrogen bypass was placed 2720 g of

9-fluorenone (15.094 moles), 5684 g of phenol (60.40 moles), and 20.60 g of 3-mercaptopropionic acid (0.1943 mole).

While kept under a nitrogen atmosphere the reaction mixture was heated to 85.8°C to effect complete solution. Forty (40.0) grams (1.096 mole) of HCl gas was bubbled into the solution and external heating was stopped. The mild exotherm carried the solution temperature to 98°C over the next 40 minutes. The reaction was heated at 90°C for 8 hours and cooled to room temperature. Solid BPF was out of solution at 90°C.

The reaction mixture was dissolved in 8 liters of methyl alcohol and filtered. The filtrate was placed in a 6-gallon container and 7.5 l of water was added with stirring. The reaction mixture was heated to reflux (84°C), to effect a clear solution, and allowed to cool slowly with seeding. The white crystals which formed were isolated by filtration, washed on the filter with 800 ml methanol/water (1:1 by volume), and dried 40 hours at 60°C and 10 mm Hg. There was much color left behind in the filtrate. No attempt was made to obtain a second crop.

The yield of white crystals was 3678.4 g, or 69.6% of theoretical yield. The product was recrystallized from nitromethane (3 g nitromethane to 1 g crude BPF) to obtain 2567.2 g, or 48.6% of theoretical yield. Concentration and recrystallization of the mother liquor yielded an additional 592 g for an overall yield of 59.8%.

1.6.2 Synthesis of Equilibrated Silicone Fluid

All glassware is flame dried, placed in a nitrogen-swept drying oven at 110°C for four hours, then in the inner chamber of a nitrogen drybox for about 15 hours. All plastic equipment is treated in a similar fashion but with flame drying eliminated. The octamethylcyclotetrasiloxane (D_4) and dichlorodimethylsilane are freshly distilled through a 2-foot Vigreaux column, under nitrogen.

A solution of 0.32 g (0.02% by weight) of $FeCl_3$, 6 H_2O, 1426.4 g (2.4 mole) of D_4, and 80.6 g (0.625 mole) of dichlorodimethylsilane was prepared by successive additions to a half-gallon bottle in a drybox; the bottle was then sealed with a polyseal cap. The bottle was removed from the drybox, covered with aluminum foil, and heated in a nitrogen-flushed drying oven for 24 hours at 48°C. The fluid was then placed back in the drybox for 24 hours and is now ready for use.

This procedure is essentially the same as described in the previous contract report[1] except for the use of flame-dried glassware and a nitrogen-flushed oven instead of a water bath at 48°C. These changes were made in the attempt to reduce the chances of hydrolysis of the product.

1.6.3 Synthesis of Endcapped Silicone Fluid

Glassware and plastic equipment were dried and placed in the nitrogen drybox as described above. Dichloroethane was stirred over $Ca(OH)_2$ for at least two days, distilled through a 2-foot bubble cap column under nitrogen, and placed in flame-dried round-bottom flasks. The BPF was dried for 48 hours at 75°C and 10 mm Hg, 24 hours in a nitrogen-flushed oven at 110°C, and placed in the nitrogen drybox while still hot.

Into a 2000-ml round-bottom flask (in the nitrogen drybox) fitted with paddle stirrer, was placed 105.1 g (0.3 mole) BPF and 900 ml dichloroethane* (freshly distilled as described above). All ground-glass joints are used without lubricant. The stoppered flask was removed from the drybox and fitted under nitrogen with a "y" gas inlet tube, thermometer, and nitrogen bypass. Ammonia (7 g, 0.41 mole) was bubbled into the slurry over a 5-minute period and a clear water/white solution obtained. (This procedure was described in the previous contract report with the exception that a one hour period was used.)

In the drybox an addition funnel, with Teflon® stopcock, was charged with 120.4 g of equilibrated dichlorosilicone fluid (previously described) and 100 ml of dichloroethane. The addition funnel was then removed from the drybox; the gas inlet tube was removed from the flask (under slight nitrogen pressure) and replaced with the addition funnel. The dichlorosilicone fluid was added to the solution of BPF-ammonia complex over a 20-minute period. A purple suspension was obtained after this addition was complete.† The temperature of the reaction went from 23 to 41°C. The reaction mixture was stirred at room temperature for one hour and then heated to reflux (81°C) for two hours; at this time the suspension was white and the solution pH was 7.1.

The reaction mixture was cooled to room temperature and 500 ml of H_2O added. The resulting solution was acidified to pH = 3.8 by the addition of 3 drops of 12 NHCl to the well stirred solution. If a clear solution is not obtained at this point, then sufficient reagent grade acetone is added.

The aqueous layer was removed by means of a 2000-ml separatory funnel equipped with Teflon® stopcock, and discarded.

The solution was washed once more with acid at pH 3.5, five times with deionized water (pH = 6.5), once with dilute $NaHCO_3$, and finally with water. The solution was then dried over $MgSO_4$, filtered, and evaporated to dryness. The residue (222 g, 103% of theory) was then redissolved in a mixture of 1580 ml of ethanol-free chloroform and 50 ml of acetone and stored in an aluminum-foil-wrapped bottle in the nitrogen drybox. (Acetone is added at this point to dissolve the BPF. Although this procedure was used in the analogous experiments described in the previous contract report, its inclusion in the report was inadvertently omitted.)

The concentrations of polymerizable BPF and linear silicone in solution were 0.06557 g/ml and 0.0705 g/ml, respectively, calculated according to the method shown on page 16 of the previous contract report.[1]

---

*The concentration of BPF in dichloroethane was reduced from that used in the previous contract report (105 g/800 ml) to maintain complete homogeneity of the BPF. The BPF-ammonia complex tends to precipitate out if less solvent is used. Heterogeneity in this reaction leads to polymers whose cast films are hazy; homogeneous conditions provide polymers which give optically clear films.

†A resultant green color at this stage requires additional ammonia. Additional ammonia was not required in any endcapped fluid preparation in the current contract work.

® Registered trademark of E.I. duPont de Nemours and Co., Inc.

1.6.4 Synthesis of BPF Carbonate-Dimethylsiloxane Block Copolymer

The glassware was thoroughly washed with acetone and dried one hour in a nitrogen-flushed oven at 110°C.

In a 5-l, 3-neck, round-bottom vessel was placed 119.5 g of BPF (0.341 mole), 1210 ml of endcapped dichlorosilicone solution [containing 0.2266 mole (79.3 g) BPF + 0.04755 mole (85.3 g) D_{15} endcapped fluid], 550 ml $CHCl_3$ (B&J ethanol free), 0.600 g (0.00638 mole)* phenol, 0.90 g (0.00413 mole) sodium gluconate dissolved in 1400 ml H_2O, and 2.00 ml (0.0143 mole) triethylamine. The stoichiometry of this polymerization reaction is designed to provide a block polymer containing 30 % by weight silicone, which corresponds to 11.6 weight % silicon.

The 5000-ml reactor was equipped with a paddle stirrer, nitrogen bypass, pH electrode, gas inlet tube, and an addition funnel containing a solution of 144 g of NaOH in 500 ml of water. This quantity of base corresponds to 300 % of the theoretical amount required to effect neutralization in the polymerization reaction. A portion of the base solution was added to the reaction mixture to obtain a pH 11, and phosgene addition was initiated at a rate of 3.5 g/h. Shortly after the addition was started a considerable amount of white solid precipitated from the mixture, and stirring became difficult. After approximately 20 % of the total aqueous NaOH had been added, stirring was considerably improved, and a homogeneous solution was observed when 50 % of the total aqeous base was introduced. Aqueous NaOH and phosgene were added simultaneously to maintain a pH of 11.0 ± 0.2.

After 60 % of the total base was consumed (elapsed time of 27 min.) the phosgene rate was reduced to 1.0 g/min and continued until the entire amount of base was consumed; this corresponded to a total reaction time of 111 minutes. Nitrogen was bubbled through the water-white two-phase system (pH 11) for 5 minutes to remove any residual phosgene. The reaction mixture was diluted with an equal volume of $CHCl_3$; the aqueous layer was separated and discarded. The organic layer was washed with deionized water (pH = 6.7), with aqueous HCl at pH = 2.0, and four times with deionized water. The last water wash was tested for chloride ion ($AgNO_3$) and pH. If chloride was present or pH less than 6.5, water washing was continued until specified limits were obtained.

The organic layer was dried over $MgSO_4$ and filtered. The resulting clear colorless solution was added over a period of 30 minutes to a well-stirred mixture of 7 l acetone and 3.5 l methanol to effect precipitation of the polymer. Prior to precipitation of the filtered solution ∿25 ml was sampled from which two films were cast by allowing the solvent to evaporate. The solution-cast film provided information about molecular weight degradation during isolation of the bulk polymer by comparison of intrinsic viscosities of the film and the precipitated polymer. Observation of the optical clarity of the film also provided an indication of the optical properties of the bulk polymer.

Following precipitation, the fibrous polymer was filtered, pressed dry, washed with a solution of 3.5 l acetone/1.7 l methanol, and refiltered. The filter cake was pressed dry on the funnel, dried at room temperature and 10 mm Hg vacuum for 20 hours, and then at 80°C and 10 mm Hg for an additional 20 hours.

*The weight of phenol constitutes a chain stopper level of 1.3 mole % based on moles of reactive BPF.

The entire polymerization, washing, precipitation, and drying are performed in a continuous operation. The polymer powder was redissolved in 1.5 l $CHCl_3$, filtered through a bed of diatomaceous earth, and then reprecipitated, washed, and dried in the manner described above.

The yield of polymer after reprecipitation was 191 g or 76.3%.

1.6.5 Melt Processing

Thermal processing of the polymer powder was done by compression molding at 350°/2000 psi and/or extrusion. For extrusion, the brabender extruder was used with a 2:1 compression screw, and a 1/8-inch rod die, at a barrel temperature of 330 to 340°C and a die temperature as much as 5 to 10° higher. As in the previous contract, feed rates were controlled with Syntron™ and K-Tron™ feeders. Starvation feeds were used until extrudate appeared; feed rate was then gradually raised to the flood condition. Problems with voiding were thus minimal.

Argon atmospheres in later extrusions were effected both in the hopper of the K-Tron feeder and in the throat of the extruder. The space between the feeder outlet and the extruder throat was enclosed. The feeds in the hopper and the barrel were purged with argon for 30 minutes before the run was started.

Compression moldings of bars 5 in. long by 1/2 in. wide by ∿1/8 in. thick for haze measurements were carried out in a stainless steel mold preheated to 350°C. The mold was flushed with argon while being loaded with resin, then closed up and placed again in the press. Following the several minutes at high pressure the mold was transferred to a water-cooled press. In most cases poor knitting of the extrudates was observed in the first molding; the bar was therefore cut in half, the two halves placed on edge, side by side, in the mold, and a second molding carried out. The twice-molded bars were usually completely knitted internally, or nearly so.

1.7 Toxicology of BPF Monomer

Preliminary toxicological screening of the BPF monomer was undertaken by the International Research and Development Corporation, of Mattawan, Michigan. The compound was evaluated for acute toxicity in rats and rabbits. Tests on albino rabbits showed the compound to be a possible eye irritant but not a primary skin irritant. Acute dermal toxicity evaluation in the albino rabbit showed that this compound was not a toxic substance by the dermal route of administration (application levels were at 200 mg and 2000 mg per kg of body weight). Oral administration of the compound at 500 mg and 5000 mg per kg body weight to albino rats under observation for 14 days did not result in death at either level. The compound is therefore not considered to be toxic by oral administration.

Contrary to some of the results of the acute toxicity evaluation described above, personnel handling BPF, particularly as a dry powder, developed skin rash near exposed moist areas of the body. The skin rash developed around the eyes, mouth, and nose, and occasionally on the hands. The rash

™ - Trademarks of FMC Corporation and K-Tron Corporation, respectively

gradually progressed to a stage resembling the skin condition produced by poison ivy. Other personnel, not involved in this project but working close to the area where BPF was handled, complained of substantial eye irritation.

The conflict between this experience and the preliminary toxicity evaluation of BPF on rats and rabbits led to further testing of the compound. Dermal sensitization studies in albino guinea pigs, using 2, 4-dintro-1-chlorobenzene as a positive control, showed BPF to be a probable sensitizing agent in man which would produce sensitization in some individuals.

Suitable safety precautions have been instituted for working with BPF, particularly with the dry material (a fine powdery material, which becomes airborne easily), so as to minimize physical contact with the compound. The difficulty in safe handling of BPF is proportional to the scale of operation.

2. CREEP

The tensile creep resistance of one of the resins made under the preceding contract (10053-152 -- 21% silicone) has been characterized over limited ranges of time and temperature. The apparatus and procedure used for this work are outlined below.

2.1 Multistation Constant-Stress Creep Tester

The apparatus used consists of six creep stations (Figure 2) mounted in an air thermostat (±1°C) together with associated data acquisitioning and processing equipment.

The specimen jigs are mounted, three over three, in a Dural aluminum frame. The top specimen chuck in each jig is connected by means of a steel rod to a flexible steel strap and thence to the short end of a lever arm. The lever arm shape is designed so that extension of the sample causes a reduction in mechanical advantage sufficient to compensate for the reduction of sample cross section, thus maintaining true stress constant. (More exactly, this design is based on the assumption that specimen extension occurs at constant volume.) The lever arm is also counterweighted so that its own weight has no influence on sample stress.

The chucks were designed for specimens approximately 0.030 in. thick and 0.5 in. wide. Blanks from which these could be obtained were compression-molded from bars of resin injection-molded under the preceding contract.

Between the bottom (fixed) chuck and the jig base a phenolic composite fixture is mounted which serves to hold in a vertical attitude a Schaevitz Engineering 250 HPD linear variable differential transducer (LVDT) coil (sensitivity = 40 volts/in.). The core is attached to a vertical brass rod screwed to a horizontal aluminum extension of the clip that is affixed to the specimen adjacent to the top chuck.

The signal from the LVDT is brought to a six-station multiplexer (Figure 3) in which the stations are sequenced at predetermined intervals. The signal from each station is fed to a digital voltmeter for digitizing, thence to a data logger, and finally to a microcomputer for storage. The Intel 8080 microcomputer also triggers data transmission from the appropriate station of the multiplexer at the appropriate time and records the elapsed time as well.

When desired, the data stored in the microcomputer memory are transferred to a magnetic tape cassette on a Texas Instrument Silent 700 terminal and thence to the central computer for processing and printout.

2.2 Procedure

After the specimens are mounted in the jigs, a series of cams (not shown in Figure 2) are rotated into position to support the lever arms. The requisite weights are then loaded on the weight pans and the thermostat chamber closed. After the desired temperature has been attained, rotation of the cams by means of extension rods that can be reached through ports in the chamber face frees the lever arms, thus starting the creep experiment.

The creep runs were carried out at stresses from 700 to 4200 psi and over times from 10^5 to 10^6 seconds approximately. (Ultimately data should be acquired out to one year, but 10^5 seconds is sufficient for assessment of general behavior.) Tests were first run at 28, then 50, and finally 80°C. Following each run the specimens were removed, inspected for cracks, crazing, and stress whitening, annealed in vacuum at 125 to 150°C, and remounted in the tester for the next run. This re-use of specimens was felt to be justifiable in view of the following:

- The anelastic portions of the creep strains never exceeded 1 % and were generally smallest at the lowest test temperature.
- No evidence of unrecoverable deformation or other damage at 28 and 50°C was seen in any case but one.
- Annealing at a temperature far above the test temperature should bring complete strain recovery.
- The scouting nature of this work.
- The a posterior evidence of another, more serious limitation, which is discussed below.

A problem reduced but not eliminated over the course of this work has been the determination of a reproducible zero-load position of the LVDT core. Although several experimental details may contribute to this problem, the most sizable error appears to arise from specimen thickness and the geometry of the specimen clip and brass rod. The specimen is thin enough so that flexing of it can easily develop when the lever arm is raised, either when the arm is raised too far and a compressive stress is developed or when under zero load the specimen exhibits a molded-in curvature. In any case, the lengths of the clip and brass rod to which the LVDT core is attached are great enough that a slight specimen flexing causes noticeable core movement. Thus, on loading, the instantaneous specimen core movement reflects both straightening and extension of the specimen. Moreover, the extraneous core movement is not reproducible with repeated loading and unloading.

Subsequent to loading, however, further core movement seems to reflect specimen extension only. Thus apparent elastic compliances are seriously in error, but creep thereafter appears to be much more uniform with time and stress level. Consequently the individual creep curves have been shifted up or down on the strain scale so that the strains at 20 seconds match the expected strains calculated from polymer moduli. (The moduli used were determined in Instron constant strain rate tests over a wide temperature range during the previous contract.) In the strain figures, only values of the strain corrected in this way are plotted.

2.3 Results

Strains corrected for the aforementioned zero-load error are plotted vs log time, in Figures 4,5, and 6, at each of the three test temperatures. The creep rates observed at 29°C are about twice those for the ICI Corporation's polyethersulfone 300P, another high-temperature glassy engineering plastic, at 20°C but are roughly 1/10 those for Plexiglas® polymethyl methacrylate at room temperature.

® - Registered trademark of Rohn and Haas Company

The creep of many materials[3] often obeys the following expression over wide ranges of stress, time, and temperature:

$$\varepsilon = At^n \exp-(E^{\neq} - \alpha\sigma)/RT \qquad (3)$$

where ε = strain

t = time

A and n = constants

$E^{\neq}$ = activation energy in the absence of stress

α = apparent activation volume.

In glassy thermoplastics far below T_g $n \leq 0.10$ usually.

Thus the data shown in Figures 4, 5, and 6 are replotted in Figures 7, 8, and 9 as log strain vs log t. The values of n derived from these plots range from 0.005 to 0.031, as expected from the fact that the T_g of the glassy matrix is so high and that no other viscoelastic loss peaks are found near room temperature in the BPF carbonate-silicone block polymer family. Figure 10 shows the influence of stress and temperature on n. The linear stress dependence seen at 28°C is reminiscent of the dependence of n on stress for polymethyl methacrylate. The fact that n is dependent on both stress and temperature tends to limit the usefulness and significance of Equation 3.

From Equation 3,

$$\frac{d\varepsilon}{dt} = \dot{\varepsilon} = nAt^{n-1} \exp-(E^{\neq} - \alpha\sigma)/RT \qquad (4)$$

and

$$\left(\frac{\partial \ln\dot{\varepsilon}}{\partial\sigma}\right)_t = \frac{\alpha}{RT} \qquad (5)$$

Thus the slopes of the well-behaved curves in Figures 7, 8, and 9 have been determined at $t=10^3$ sec and plotted vs stress on a semilog plot (Figure 11).

The dependence of the 28° data on stress is reasonably linear. Data at the higher temperatures show similar behavior.

The lack of much temperature dependence of creep rate at a given stress is noteworthy. This lack implies a low-creep activation energy. No attempt was made, however, to extract activation parameters from these data. For this to be done with any accuracy creep studies will have to be extended to higher temperatures.

Two of the specimens at high stress (2800 and 4200 psi) failed in a brittle manner in the last decade of the run at 80°C. On subsequent dismantling of

3. R.P. Kambour and R.E. Robertson, "The Mechanical Properties of Plastics," Polymer Science, Vol. I (A.D. Jenkins, ed.), North Holland Publishing Co., Amsterdam, Netherlands, 1972, Ch. 11, pp. 687-822.

the apparatus, all specimens were inspected. No other evidence of damage (crazing, stress whitening) was seen. On dismantling at 50°C the specimen at 4200 psi showed a single craze in the middle of the test section and a small wedge-shaped area of intense stress whitening at the edge radius where the test section and specimen grip section join. (The stresses here are complex.) Otherwise no specimen damage was seen in the 50°C or 28°C tests.

It was also noticed that oil, presumably volatilized from the fan motor, had condensed on the faces of the thermostat. It is conceivable that the crazing and brittle failure of the specimens at the higher temperatures was induced by this oil.

3. CRAZING RESISTANCE

Injection- and compression-molded specimens of block polymer 10053-152[1] (21 % silicone) have been subjected to tests of craze resistance under constant strain in air at room temperature. The first specimen was one of the compression-molded blanks from which the creep specimens were cut. The second and third were injection-molded bars 1/8 in. by 1/2 in. by 2-1/2 in. long.

All three were strapped down to Bergen elliptical strain jigs. Maximum strains induced in these specimens were approximately 3.5 % (compression molded) and 5.0 % (injection molded).

No crazing or cracking occurred in these specimens in five months under strain.

As noted in Section 2, "Creep," specimens of this resin subjected to a constant stress of 4200 psi for times of 10^5 to 10^6 seconds exhibit no crazing or cracking at 28°C. At 50° and 80°C the critical stress for crazing and cracking appears to be approximately 4000 psi.

This resin therefore exhibits a crazing resistance in air superior to that of most commercial transparent thermoplastics (e.g., see Table 6).

TABLE 6

Critical Stresses (σ_c) and Critical Strains (ε_c) at Room Temperature for Several Glassy Polymers*

Polymer	ε_c(%)	σ_c(psi)	$t_{max,\varepsilon}$(hr)†	E (psi)	σ_y(psi)±	T_g(°C)
Polystyrene	0.35	1600	24	440,000	10,000	90
Poly (methyl methacrylate)	0.8, 1.30	~3500	100,0.1	425,000	~13,000	100
Poly (2, 6-dimethyl-1, 4-phenylene oxide)	1.5	--	~24	380,000	10,500	210
BPA polycarbonate	1.8	--	~24	340,000	8,500	145
Polysulfone	2.5	--	~24	360,000	10,000	185
Styrene-acrylonitrile	0.49	--	~24	450,000	--	90
BPFC/DMS resin 10053-152	>4.5	>4200	~700	260,000	8,000	~210

† For constant strain tests.

± Tensile yield stress for shear yielding.

* Data for all resins except BPFC/DMS taken from ref. 4: R.P. Kambour, "A Review of Crazing and Fracture in Thermoplastics," Journal of Polymer Science, Part D, Macromolecular Review, Vol. 7, 1973, pp. 1-154.

4. FLAMMABILITY PROPERTIES

A number of tests have been conducted to explore further the flammability characteristics of the BPF carbonate-silicone block polymers and to attempt to understand the synergism in flame resistance operating between the BPFC and the DMS blocks.

4.1 Limiting Oxygen Index

The Fenimore-Martin limiting oxygen index (LOI) test (ASTM Test No. D2863-70) was run again on the homopolycarbonate and on a block polymer containing 7 % silicone, in order to better define the dependence of LOI on silicone content. The results of these tests and those run in previous contracts are summarized together in Table 7 and plotted vs silicone content in Figure 12. These results show that no further increases in LOI are to be obtained by increasing silicone content above 15 %, at least in the unadulterated block polymers.

4.2 Smoke Density

Smoke density measurements were made on 3 in. by 3 in. by 1/8 in. plaques of two resins in a National Bureau of Standards smoke chamber. The plaques used were compression-molded from sprues and runners of block polymers 10053-136c and 10053-151, produced in the injection molding trials in the previous contract. The tests were run in the so-called "flaming condition." The smoke density, D_m, is the maximum optical density, D, reached in the chamber during the period of the test (20 min):

$$D = 132 \log_{10} \frac{100}{T(\%)}$$

T = optical transmittance

D(corr) is obtained by correcting D for the soot on the windows of the light source and photocell.

The results are listed in Table 7. These resins are considered to be "good" (i.e., smoke production is relatively low) as flame-resistant plastics go. Smoke densities built up slowly, reaching their maximum values in about 20 minutes. During the tests, specimen surfaces charred extensively. Little puffs of white smoke were emitted intermittently from the specimen during the tests. Substantial outflow of resin from underneath the char at the bottom of the plaque was also noted at the end of each test. Upon removal of the plaque from the holder, the center of each plaque underneath the char was found to have flowed away completely.

4.3 Thermogravimetry

Thermogravimetric analysis (TGA) was extended to include pure silicone gum and block polymers of 7 % and 50 % silicone (these are, respectively, resin 9824-97B-X and a leathery block polymer made outside the contract). The thermograms of these and previous runs are superimposed in Figures 13 and 14. The residues at 700°C from the runs in air are always white; usually the residue consists of a number of coarse transparent pieces partially stuck together.

TABLE 7

Flammability Characteristics of BPF Resins

Resin	Silicone Content (%)	LOI†	D_m^* (corr)
BPF Polycarbonate	0	38 - 40	
9824-97B-X**	7.5	45.0 - 45.7	
9824-101A-X**	8.7	50.3	
10053-129B[1]	23	48 - 49	
10053-132c[1]	24	49.1 - 50.2	
10053-136C[1]	21.5	49.8 - 50.3	70.5
10053-151[1]	16	50.3 - 51.1	80.5

†ASTM limiting oxygen index.
*Maximum smoke density, flaming condition
**Made under first contract. (Ref. 5: R.P. Kambour and G.E. Niznik, Synthesis and Properties of Bisphenol Fluorenone Polycarbonate and BPF Carbonate-Dimethyl Siloxane Block Polymers, Final Report, Contract N00019-73-0152 for the Naval Air Systems Command, Department of the Navy, January 1974.)

With the 50 % silicone resin the residue was a single, hard, transparent piece. These residues are undoubtedly SiO_2, probably in a state of low crystallinity. (The suboxide SiO apparently does not form at these temperatures, even under reducing atmospheres. Moreover, it is a brownish or yellowish solid, readily oxidized to SiO_2.) The previously noted dependence of the amount of air-TGA residue on silicone content is confirmed in Figure 15, where all air residue data from this and prior contract investigations are plotted vs block polymer silicone content. The theoretical line is based on the assumption of a quantitative conversion of silicone to SiO_2. As with LOI, a synergism in air-TGA residue production is seen, a synergism most strikingly evident at 50 % silicone where the conversion of silicone to SiO_2 is still 80 % of theoretical. The contrast is further enhanced by the fact that the nitrogen-TGA residues at 700°C decrease linearly with silicone content, extrapolating to zero at 100 % silicone (Table 8 and Figure 16).

TABLE 8

TGA (N_2) Residues at 700°C

Resin	% Silicone	TGA Residue-N_2 (%)
PBPFC	0	64
-129B	23	55
132C	24	58
136C	21.5	58
151	16.3	60
50/50	50	34
97B-X	7	64.5
101AX	8.7	61
93A	27	49

Finally, a nitrogen/air sequential run was carried out on the 50 % silicone block polymer. Following a standard TGA run in nitrogen to 780°C, the atmosphere was changed to air and the temperature held constant until no further weight loss occurred. During the latter part of the run the residue weight changed from 37 to 9 %. The final residue weight stands in marked contrast to the 29 % residue obtained when the TGA atmosphere was air throughout the run (see Figure 15).

4.4 Char Characterization

Char formation and stability are key aspects of flame resistance. Consequently, chars formed in the oxygen index test and other burning tests have been the subject of several observations and tests.

4.4.1 Volume and Density

The thermal insulation provided underlying resin by its char will depend on char thickness and density. Attempts have thus been made to characterize the weight and volume of char produced in burning tests.

First the dimensions of the completely charred sections of LOI bars of BPF polycarbonate and resin 10053-136C were compared. Respective cross-sectional areas increased by factors of 2 and 2.9 very roughly.

The weight of char produced in the LOI test has not been determined because only a portion of the specimen is burned in the test.

In a separate experiment, molded pieces of homopolymer and block polymer 10053-132c were placed in aluminum pans under a radiant heat source, in air, for three minutes. The specimens swelled strongly upon heating, becoming rather smooth hollow shells, rather like balloons. Balloon volume was at least five times the original specimen volume. The balloons expanded under internal gas pressure, developed leaks and shrank somewhat, then healed and began the expansion process again. At high temperatures they exhibited a somewhat elastomeric character; upon cooling they were black and brittle. Residues of uncharred resin were found afterward inside the bases of the char balloons. The char yields (ca. 65 % for both resins) calculated from weights before and after the test are somewhat high. The fact that no flaming occurred during the test reflects a local atmospheric oxygen content much lower than that in the LOI test.

By contrast with these chars LOI chars show much less tendency to trap volatiles, expand strongly, leak, or contract; rather, LOI chars are porous foams. In short, the physical character of the char seems to depend substantially on the atmosphere in which it is formed. Presumably temperature and oxygen content of the atmosphere are the controlling factors.

4.4.2 Char SiO_2 Content

The oxygen content of the atmosphere at the surface of and/or within the LOI char presumably controls the extent to which silicone is converted to SiO_2 in the char instead of being lost through volatilization. Conversely, a measurement of SiO_2 content of LOI char may suggest the extent to which this atmosphere is like that of TGA tests run in air or nitrogen.

Thus samples of LOI char from several block polymer resins were digested in aqueous hydrofluoric acid (this converts SiO_2 to SiF_4, which volatilizes*). Weight losses of 7 to 19 % occurred (Table 9). These results suggest that the atmosphere at or in the LOI char contains enough oxygen to produce conversion of much of the silicone to SiO_2. (Just how much is not clear since exact char yield is not known.)

TABLE 9

Weight Loss from LOI Chars as a Result of HF Digestion

Resin	Original Silicone Content (%)	Weight Loss (%) from Char
9824-101A-X	9	7.2
10053-132C	24	11.3
10053-136C	21.5	15.7
10053-151	16	18.7

4.4.3 Microscopy

A piece of LOI test char from resin 10053-136C was inspected by scanning electron microscopy (Figure 17). Subsequently the piece was vacuum-impregnated with epoxy. Following cure of the mounting resin the specimen was petrographically thinned and polished to produce a section normal to the long axis of the original LOI char. The section was inspected by light transmission microscopy and subsequently by scanning electron microscopy (SEM)/electron microprobe analysis, in an attempt to find a SiO_2 phase.

In transmitted light (Figure 18) the foamy character of the char is evident. It is also notable that the char can be divided into two regions -- a thin outer shell through which no light can be passed and the remainder, which appears yellow to dark brown, depending on thickness. The outer black shell presumably has no polymeric character remaining. The inner, light-transmitting portion has not carbonized and thus may still bear a resinous character, albeit not enough to be soluble in chloroform.

SEM micrographs formed by using plate current and silicon x-ray emission intensity to modulate cathode ray tube beam intensity are shown in Figures 19 and 20, respectively. Silicone x-ray emission is uniform throughout the char; therefore no separate silicon-rich phase is observable at this level of magnification. (X-ray emission from silicon is low enough to preclude inspection at higher magnification.)

4.4.4 Transmission Electron Microscopy

Subsequently, another molded bar of 10053-136C was partially burned at 50 % oxygen in the LOI tester (Figure 21a). Following epoxy-mounting, the charred end of the bar was sawn in half on a plane that included the long axis of the bar. Ultrathin sections were microtomed from two internal regions and a surface region of the char as shown in Figure 21b.

*Any remaining silicone would also react; the products would also tend to cyclize and evaporate.

The sections were backed with carbon and examined in a Siemens ELMISKOP 101 transmission electron microscope. Figure 22 shows part of region 1 of Figure 21b; the region contains well-dispersed spheroidal globules roughly 2.5 μm in diameter throughout. These are apparently responsible for the intense light scattering from region 1. The globule seems to be softer than the matrix, as evidenced by the way the cutting-induced compression of the matrix has caused the globules to bulge. Each globule also seems to evidence a nodular morphology, the nodule diameter being roughly 0.1 μm (Figure 23).

The composition of the globules is unknown. Both globule and nodule diameters are much greater than the diameters of the silicone microdomains of the undamaged resin. The volume of the globules is estimated to be 20 to 30 % of the total in region 1. Perhaps fortuitously, this corresponds to the volume of silicone in the block polymer. Such a correspondence leads to the speculation that the resin in region 1 may have broken down sufficiently for a reagglomeration of silicone-rich material to have occurred on a macroscale.

Region 2 (Figure 24) contains large numbers of small, electron-dense particles scattered throughout. However, none of the globules seen in region 1 are evident here. The shapes and electron densities of these particles are suggestive of fumed silica. Since the particles do not diffract electrons, a positive chemical identification has yet to be made.

Region 3 spans the external boundary between char and epoxy. The char half of each ultrasection from region 3 also contains internal pockets of epoxy. These pockets are presumably cross sections of channels which are connected at other depths to the external char surface. (Without these connections they would not have been filled with epoxy.) The external boundaries are defined only by the abrupt drop in particle frequency to zero (Figure 25). The surface of each internal channel is additionally defined by a continuous lining of electron-dense material 0.1 to 1.0 μm thick (Figure 26). Many of these epoxy pockets also have internal subdivisions formed by layers of the electron-dense material (Figure 27).

The internal surface layers respond to the microtome knife in a way reminiscent of other, very brittle, substances (Figure 28). Neither the layers nor the particles give rise to electron diffraction. Raising the electron beam intensity to its maximum caused complete erosion of the epoxy and the char matrix, leaving the layer and the particles unchanged (Figure 29). Thus, the particles and the surface layers are electron-dense, friable, heat-stable, and amorphous. These observations support, but do not prove, the hypothesis that the particles and surface layers are glassy SiO_2.

4.5 High-Temperature Chemistry

Attempts have been initiated to analyze the chemical changes occurring in the BPF resins in an air stream over the temperature range from 350 to 600°C. The primary aim of these studies was to determine the fate of the silicone blocks. Specifically, does chemical evidence support the supposition that the silicone in the resin becomes converted to a siliceous phase before the BPFC block is completely oxidized?

Two experiments were carried out. In the first a single specimen of block polymer was heated at a number of successively higher temperatures, ten minutes

at each temperature. The volatile organic and organosilicon products of each stage were trapped and analyzed subsequently by gas chromatography/mass spectrometry.

In the second experiment a number of fresh specimens of block polymer and one of homopolymer were each held for ten minutes in air streams at one fixed temperature. After this single high-temperature exposure each specimen was extracted with chloroform. Weight loss and the weight of extractable material produced in each specimen were determined. The insoluble fraction is considered to be a network held together by chemical bonds of various currently unknown kinds. The two experiments and the results from them are described below.

4.5.1 Volatile Products

A specimen of 10053-132c block polymer powder was suspended in a plug of glass wool in a quartz U-tube. The upstream side of the tube was connected to an air line. A Tenax collector tube was fitted to the downstream end of the quartz tube. (The Tenax tube contains a temperature-stable particulate resin (poly-2, 6-diphenyl-1, 4-phenylene oxide) which absorbs organic vapors. The resin absorbs CO_2 to some extent and water to a very small extent.)

The U of the quartz tube was inserted in a furnace at 400°C for 10 minutes. At the end of this time, the tube was removed from the furnace, the Tenax tube replaced by a new one, the furnace temperature raised to 450°C, and the U-tube reinserted. This process was carried out at 400, 450, 500, 550, 575, and 600°C in an attempt to reproduce most of the TGA (air) decomposition process for this resin. Visual observations were made throughout the run. These are recorded in Table 10.

TABLE 10

Observations During Stages of Heating
of Block Polymer 10053-132C* in Air Stream

T(°C)	Remarks
400	During first 5 minutes effluent contained a white fog or smoke not believed to be H_2O. Brownish condensate deposited in tube at exit from furnace throughout time period. First part of Tenax tube also became yellow-brown. On removal of tube from furnace resin appeared dark-brown and foamed. A little dark-brown deposit at tube bottom.
450	First part of Tenax tube became slightly brown. On removal of tube residue was almost black. More brownish condensate at tube bottom and at furnace exit.
500	White smoke seen in effluent from 2 to 5 minutes. On tube removal white powdery deposit seen in tube just prior to exit from furnace. Sample residue brown-black in color and much reduced in volume.

*Dried *in situ* 2 hours at 150°C.

TABLE 10 (Cont'd)

Observations During Stages of Heating
of Block Polymer 10053-132C* in Air Stream

T(°C)	Remarks
550	Nothing seen during heat. On tube removal most of sample was gone. Remainder a light yellow powder. Brownish condensate at furnace exit appeared to contain needlelike crystals.
575 and 600	Gradual whitening of residue. Otherwise no observable changes.

*Dried *in situ* 2 hours at 150°C.

Subsequently a portion of the powder from each Tenax tube was heated at a programmed rate in the specimen chamber of a Varian GC/MS System MAT 111 gas chromatograph/mass spectrometer. Effluent from the gas chromatograph was sampled to the mass spectrometer at appropriate intervals. Sampling frequency was high in the "spikes" of the GC recorder trace, indicating the passage of one or more compounds out of the end of the GC column. In all more than 600 mass spectra were obtained.

A very large number of products were trapped by the Tenax tubes (more than 80 products from the 400°C heat alone). The amounts of these compounds varied widely. Only the major ones have been identified. GC peak heights were measured or estimated for all of the major compounds at each temperature (Table 11). (Saturation of the detector occurred in several cases, making possible only semiquantitative determination of peak height in these cases.)

GC peak heights for the major products are plotted vs temperature in Figure 30. Peak height depends on both amount of compound and detector sensitivity; the latter factor varies from one compound to the next. Thus peak heights for different compounds should be compared only for gross differences. Another factor limits to a degree the accuracy of comparison of peak heights for a given compound. For the lower temperatures only a fraction (e.g., the first 1/3) of the Tenax tube absorbent was placed in the GC sample chamber; for higher temperatures, where the number of volatile products was small, 2/3 or all of the absorbent was used. The method of sampling the lower-temperature Tenax tubes precludes calculating a quantitative scaling factor with which to adjust peak heights for sample size variation.

In spite of the limitations cited above, two major trends are evident in Figure 29:

- Production of cyclics from the silicone blocks decreases rapidly above 400°C.
- Production of organic volatiles by reaction of the BPF block peaks at 450°C. (Although not shown here, CO_2 evolution is strongly maximized at 500°C.)

TABLE 11

Major Volatile Products from Thermooxidation of Block Polymer 10053-132c at Successively Higher Temperatures

Compound	Peak Height (Arbitrary Units) at T(°C) = 400	450	500	550	575	600
A. Silicones						
Cyclic tetramer (D_4)	12	1.6	1.8	0	0	0
Cyclic pentamer (D_5)	32	2.8	0	0	0	0
Cyclic hexamer (D_6)	≈100	2	0	0	0	0
Cyclic heptamer (D_7)	≈100	~30	0	0	0	0
1-phenyl, 2-hydroxytetramethyl disiloxane	3	10	2	0	0	0
B. Others						
Carbon dioxide	11	13	≈100	7	5	7
Phenol 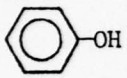	~60	~60	20	0	0	0
P-cresol 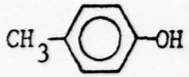	5	8.5	0.3	0	0	0
Biphenyl 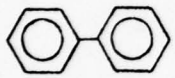	24	~75	10	0	0	0
Dibenzofuran 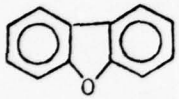	12	≈80	~40	3	4	3

TABLE 11 (Cont'd)

Major Volatile Products from Thermooxidation of Block Polymer 10053-132c
at Successively Higher Temperatures

Compound	Peak Height (Arbitrary Units) at T(°C) = 400	450	500	550	575	600
B. Others (cont'd)						
Diphenyl ether						
or hydroxy biphenyl	0	7	1	0	0	0
Fluorene	6	20	7	0.3	0.5	0.5
Fluorenone	11	≈100	16	2	5	5
Xanthone						
or benzcoumarin	2	6	3	2	1	0.4
or hydroxy fluorenone						
Benzofuran	0	3	5	0	0	0

TABLE 11 (Cont'd)

Major Volatile Products from Thermooxidation of Block Polymer 10053-132c
at Successively Higher Temperatures

Compound	Peak Height (Arbitrary Units) at (T°C) = 400	450	500	550	575	600
B. Others (cont'd)						
Quinone 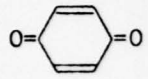	0	3	2	0	0	0
3-vinyl furan 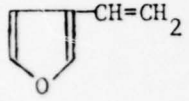	0	?*	5	0	0	0
Anthracene (and/or isomers) 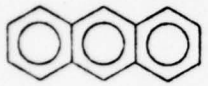	0	0	0	0	1	4

*Masked largely by phenol peak.

At first glance, three possible causes are seen for the reduction in the amount of silicone cyclics found in the Tenax tubes with increasing temperature:

1. So much silicone is volatilized at 400° that little is left to be volatilized at 450 and 500°C.
2. Silicone continues to be cyclized at a high rate at the higher temperatures but becomes oxidized in the air downstream from the sample and precipitates out as SiO_2.
3. The same as 2 except that SiO_2 formation occurs in the char, as suggested by the electron micrographs.
4. The silicone block undergoes a reaction *in situ* (e.g., CH_3 oxidation followed by Si-O-Si crosslink formation) that prevents cyclization.

The first of these possibilites is ruled out by the fact that a substantial amount of a white solid (presumably SiO_2) was seen in the original sample location at the end of the experiment (Table 10). The second seems highly unlikely for the same reason; although a white smoke was seen emerging from the furnace and a powdery white solid seen to precipitate on the tube wall just outside the furnace, the total quantity of solid produced was small compared to the amount left in the original sample location.

The third and fourth possibilities remain: cyclization, transport through the char to outer regions, reaction there with oxygen, and precipitation; or *in situ* CH_3 oxidation followed by Si-O-Si crosslink formation between neighboring blocks.

Two other features of these results are worth noting. First, very little cross-product between the two kinds of blocks was identified; this suggests that except for cyclization retardation by the BPF block the block polymer's high-temperature chemistry is largely the sum of the high-temperature chemistries of BPF polycarbonate and a highly crosslinked silicone resin. Such behavior would make the analysis of the flammability synergism in silicone block polymers much easier.

Second, one of the major volatile products from the BPF block, dibenzofuran, is a first cousin of an extremely toxic substance, dichlorodibenzofuran. Great caution should therefore attend any future R&D effort in which chlorine-containing substances (e.g., many of the commercial retardants) are combined with BPF-containing substances with an eye to producing flame-resistant materials. Chlorination of the BPF rings in high-temperature degradation experiments or in fires, should such occur, could have serious toxicological consequences.

4.5.2 Gel Formation

BPF polycarbonate batch 9824-78A and BPFC/DMS block polymer batch 10053-132c were used in virgin state (fibrous and granular morphology, respectively) in the assessment of resin insolubilization at high temperature. Teflon-coated aluminum foil was fashioned into "boats" about 1/4 in. by 1/4 in. by 1 in. long. Each was loosely filled with resin and then inserted in a tube at high temperature. Airflow rate through the tube was 0.04 ft^3/min. After ten minutes, the boat was removed from the tube. The residue in the boat was transferred to fine-mesh wire screen, wrapped tightly, and placed in the cup of a Soxhlet extractor.

Extraction in refluxing chloroform was carried out for 3 to 4 hours. The screen was then removed and dried in a vacuum oven for 1/2 day.

Appropriate weighings during this procedure allowed calculation of the loss in weight and the extent of development of insoluble components in the specimens (Figure 31). Two aspects of the results are noteworthy. First, substantial but equal amounts of gel form at 350°C in the two resins. Second, the block polymer develops much more gel at 400 and 450°C than does the homopolymer. It is therefore inferred that extensive reaction of the silicone to produce insoluble material occurs at 400°C.

Along with increased gel formation a decrease in weight loss is seen in the block polymer at 400 and 450°C.

The two resins seem to behave in a similar manner again at 500°C. However, this may be more apparent than real. Foaming of these specimens was so vigorous that substantial spillover into the tubes occurred; not all the material that stuck to the tubes could be scraped off. Moreover the Teflon of the aluminum boats showed signs of degradation. Finally, some of the Teflon stuck to the sample residues when the latter were removed from the boats. Thus the results at 500°C are suspect.

4.6 Discussion

These results, taken together, indicate the following:

a. The resistance ranking of a BPFC/DMS resin to high-temperature breakdown and burning is dependent on atmospheric oxygen content and temperature. The higher the oxygen content, and probably the higher the temperature or the faster its rise, the better will the block polymers appear to be relative to BPF polycarbonate.

b. Silicone contents of 15 to 20 % are sufficient to maximize flame resistance as measured by the oxygen index test. However, it should be remembered that the silicone blocks in the resins tested to date have all been about the same length. Perhaps a more important caveat relates to the LOI test itself. The use of oxygen enrichment of the atmosphere is well recognized to be an inaccurate substitute for elevating atmospheric temperature. In contrast with LOI conditions, the atmospheres in the presence of fires have temperatures higher than 25°C and oxygen contents equal to or less than 20 %.

c. The mechanism of flame-resistance enhancement probably hinges on thermal insulation by the char of the underlying unburnt resin.

d. The increase in thermal insulation probably involves the increased volume of char afforded by block polymers.

e. The increased char volume probably results either from increased foaming at high temperature by the volatile products from the silicone blocks or, more likely, from the protection of char against further oxidation by the deposition on the surfaces of the char pores of a siliceous layer. The chemical and physical steps in the conversion of the silicone blocks to siliceous layer are not known.

f. The retardation of silicone cyclization and volatilization by the BPFC blocks allows the silicone to remain in the specimen until oxidation occurs. (Similar retardations of cyclization have been previously reported [6,7,8,9] for other silicone copolymers in each of which the other component a) has high temperature stability but b) cannot be incorporated in a volatile, silicone-containing cyclic.) Silicone oxidation occurs at temperatures below the range where most of the BPF breakdown occurs. Thus the flame-resistance synergism appears to require a thermooxidative stability in the organic block sufficient to preserve the silicone up to its oxidation temperature.

g. BPFC char is copious and thermally stable in the absence of oxygen. Thus the siliceous layers provide the atmospheric protection necessary for high temperature stability.

In regard to future research in this area, there are still a number of unanswered questions as well as several speculations that are worth setting down:

1. What are the chemical details of the silicone oxidation?
2. To what extent in a flame test does silicone become converted to SiO_2 *in situ* on a microscale? Conversely, how much silicone undergoes cyclization followed by transport in the gas phase to a hotter and/or more oxygen-rich region of the specimen, and only there undergoes oxidation? Such a process would tend to turn a specimen inside out as char formation proceeded. The hollow form of the char and the lining of the outer pores by a continuous, presumably siliceous coating suggest that this inversion actually occurs.
3. Could an additive consisting of a silicone elastomer containing well-dispersed, very short BPF blocks raise flammability resistance of BPF polycarbonate to the level of these block polymers?
4. Would the LOI's of thermoplastics exhibiting low thermal and/or thermooxidative resistance (e.g., polystyrene) and/or little char formation on burning (e.g., polymethyl methacrylate) be unchanged by silicone block incorporation?

It seems likely that a more thorough understanding of the chemistry, morphology, and physics of resin degradation and char formation will be required for fabrication of a complete model of the silicone flammability synergism.

---

6. V.V. Korshak and S.V. Vinogradova, Usp. Khim.,Vol. 11, 1968, p. 2024.

7. W.R. Dunnavant, Inorg. Macromol. Rev., Vol. 1, 1971, p. 165.

8. P.C. Juliano and T.D. Mitchell, Novel Block Copolymers, Report No. AFML-TR-73-171, Part II, for the Air Force Materials Laboratory, Department of the Air Force, Aug. 1974.

9. I.J. Goldfarb, E. Choe, and H. Rosenberg, American Chemical Society Coatings and Plastics Preprints, Vol. 37 (1), 1977, p. 172.

5. ACKNOWLEDGMENTS

The authors wish to acknowledge the help of E.M. Lovgren, R.L. Reis, and S. Smith with melt processing and haze measurements, and of R.B. Bolon, D.G. Fink, A.S. Holik, and R.R. Russell with microscopy. The assistance of D.H. Wilkins in analyzing TGA results and the discussions of flammability with J.C. Carnahan, A. Factor, and M.R. MacLaury were also of considerable help. Finally, we wish to thank W.V. Ligon, who carried out the GC mass spectroscopy analysis.

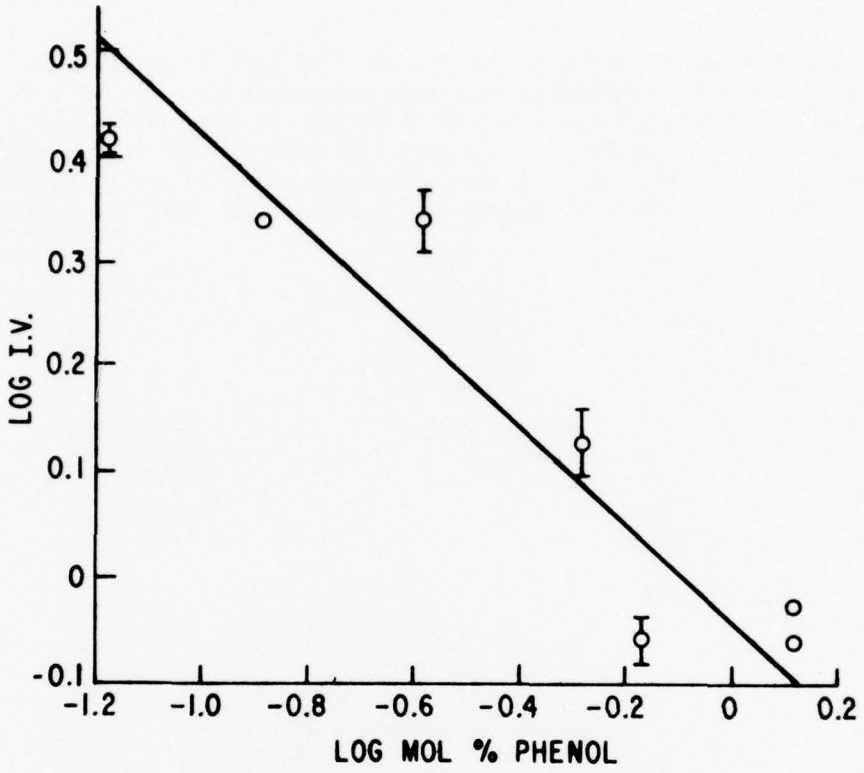

Figure 1. Dependence of intrinsic viscosity [η] of resin powder on chain stopper (phenol) concentration in reaction mixture.

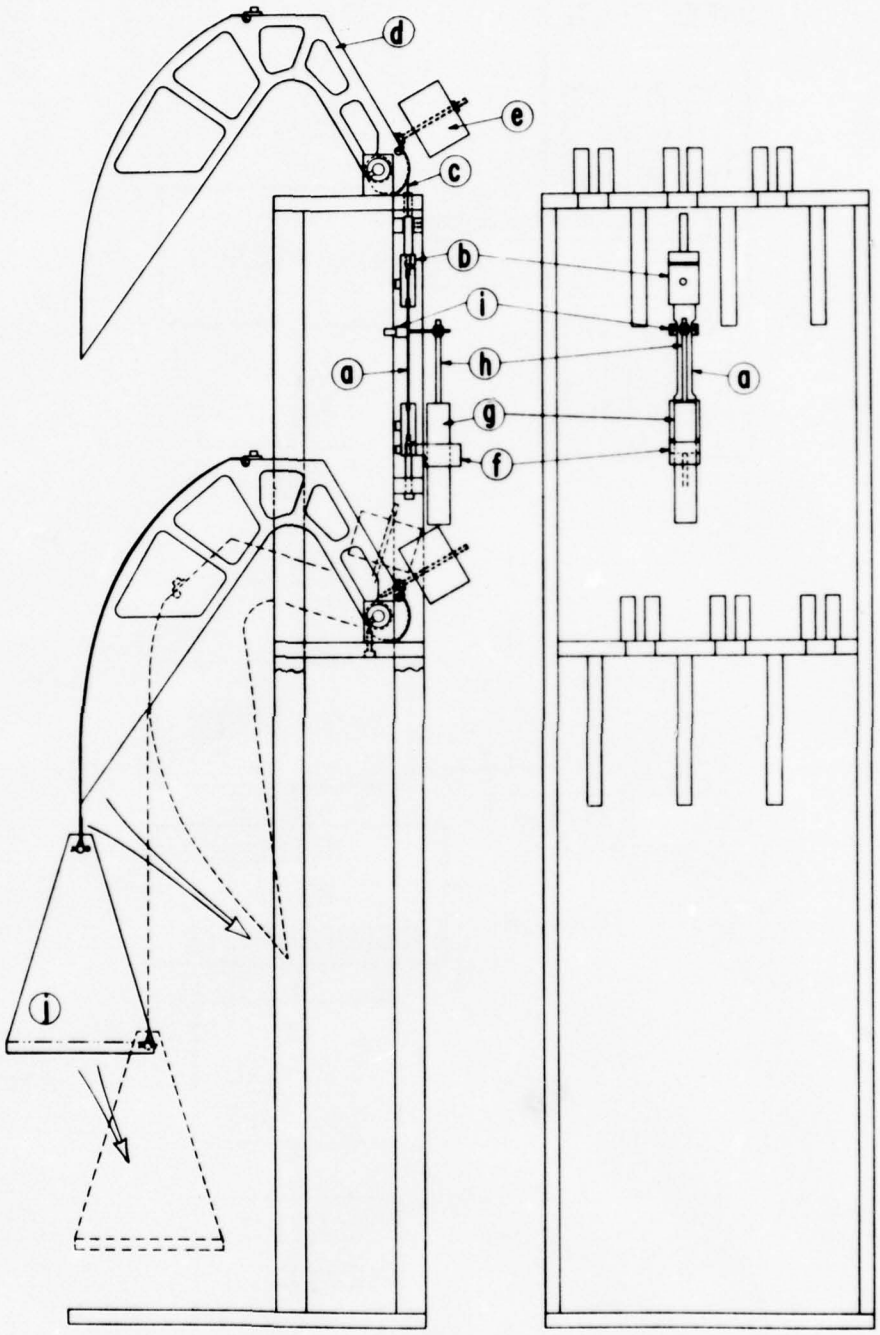

Figure 2. Six-station creep tester: a) specimen, b) upper chuck, c) steel strap, d) lever arm, e) counterweight, f) phenolic composite fixture, g) LVDT coil, h) brass core extension rod, i) clip connecting LVDT core to specimen, j) weight pan.

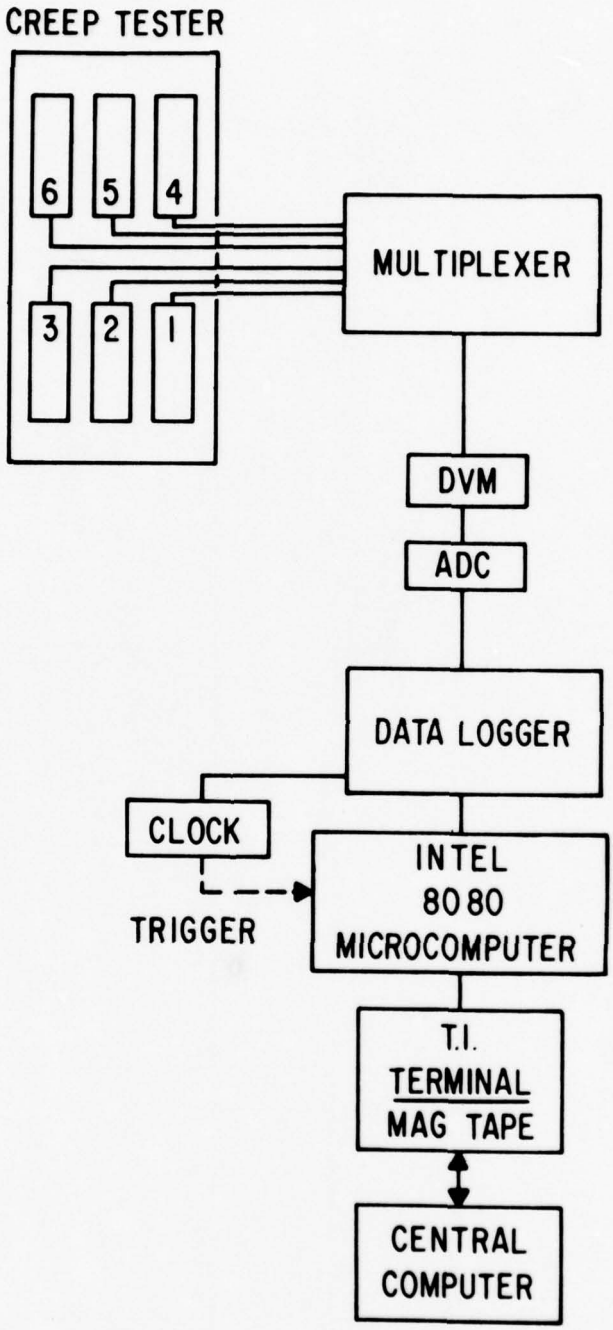

Figure 3. Schematic diagram of creep data acquisition and processing equipment.

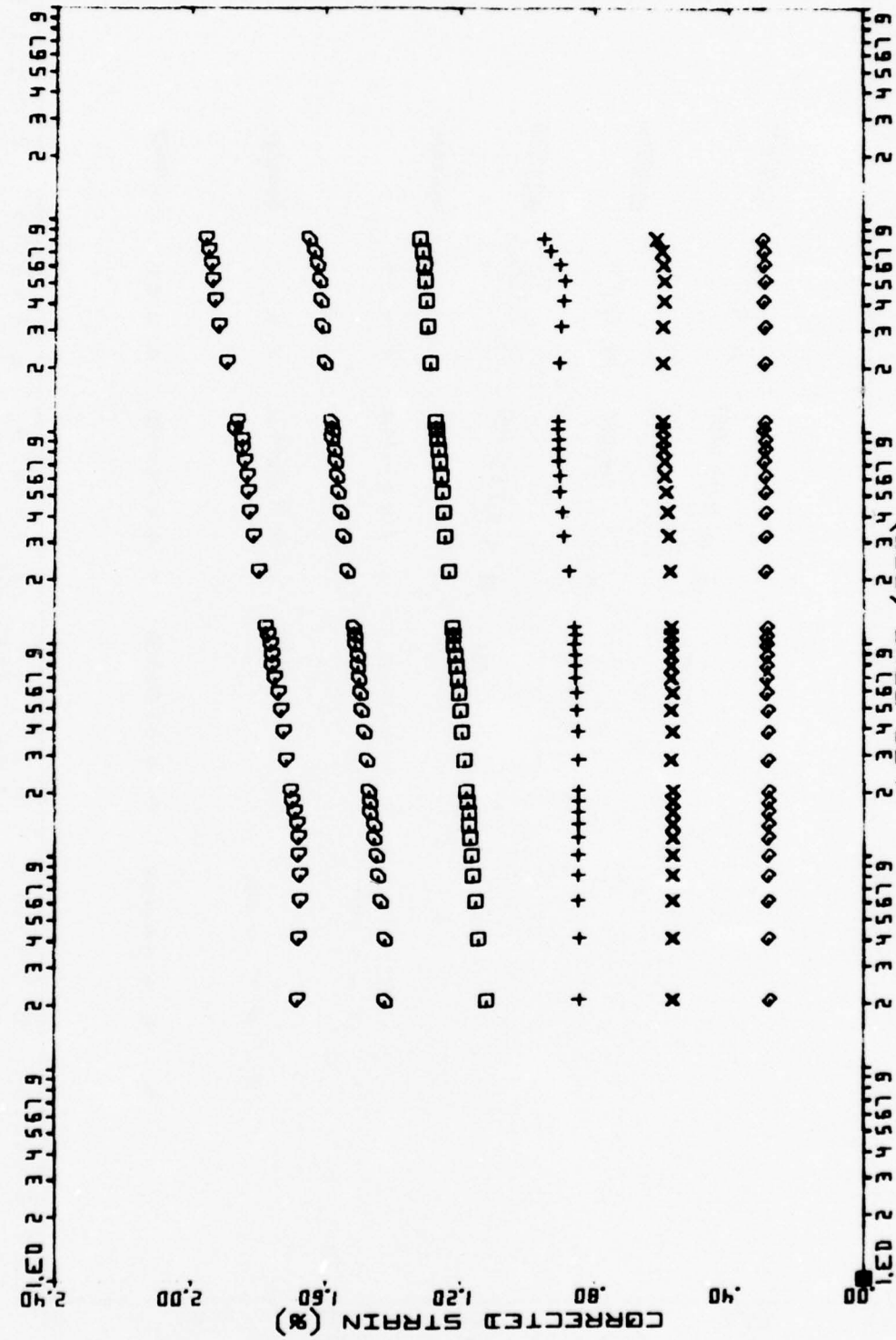

Figure 4. Creep behavior at 28°C and several stresses in ascending order: 700, 1400, 2100, 2800, 3500, and 4200 psi.

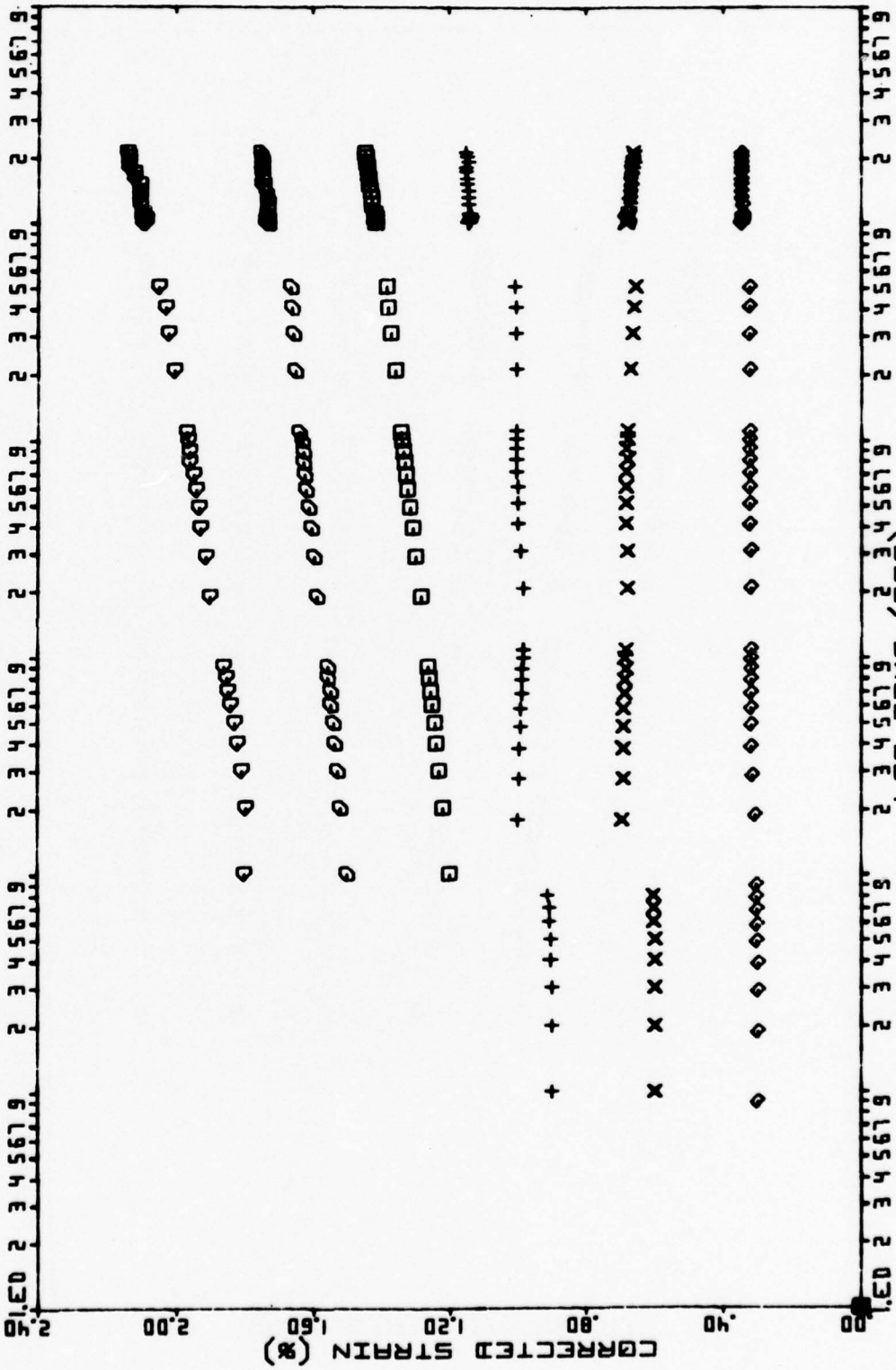

Figure 5. Creep behavior at 50°C. Stresses are same as in Figure 4.

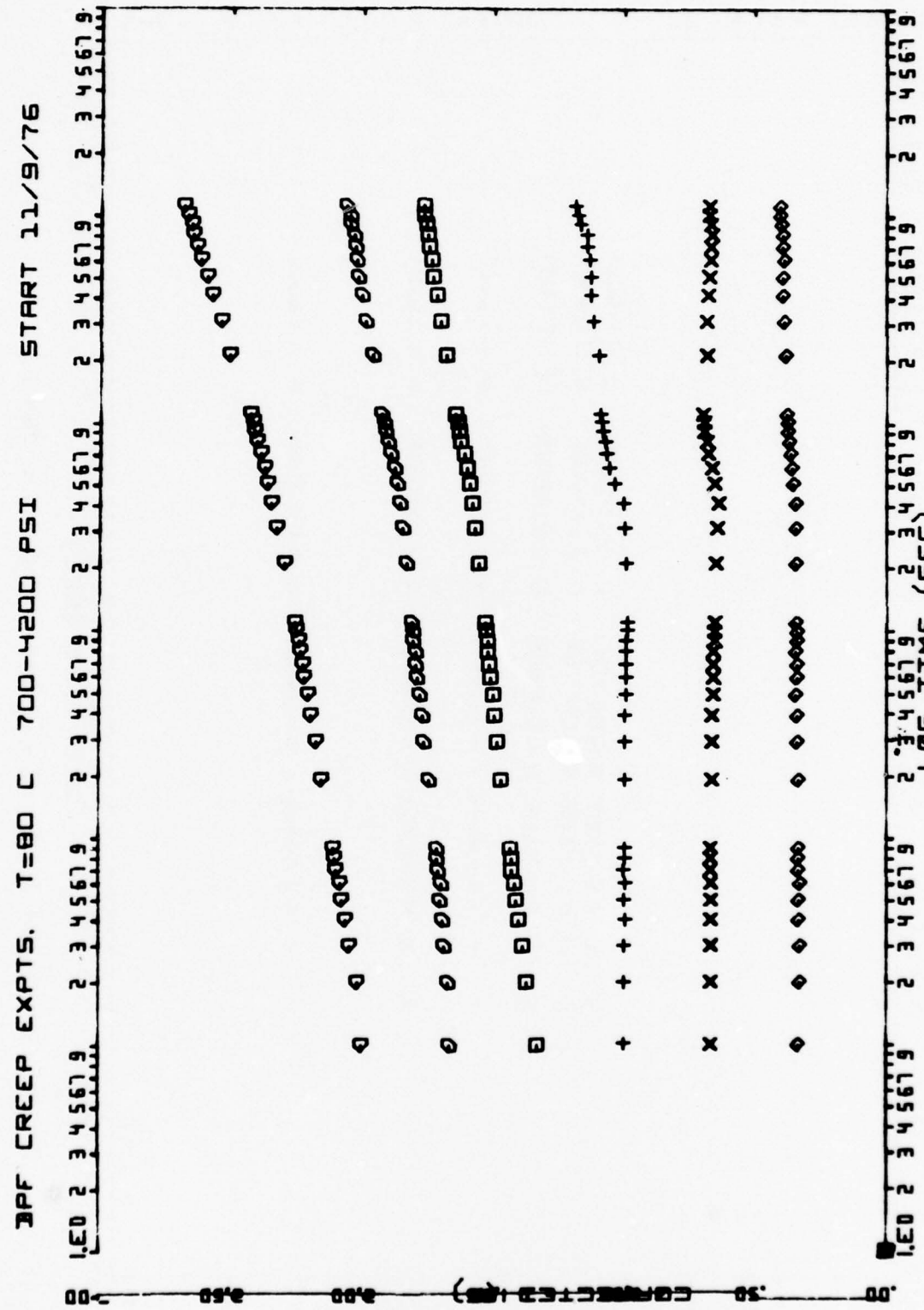

Figure 6. Creep behavior at 80°C. Stresses are same as in Figure 4.

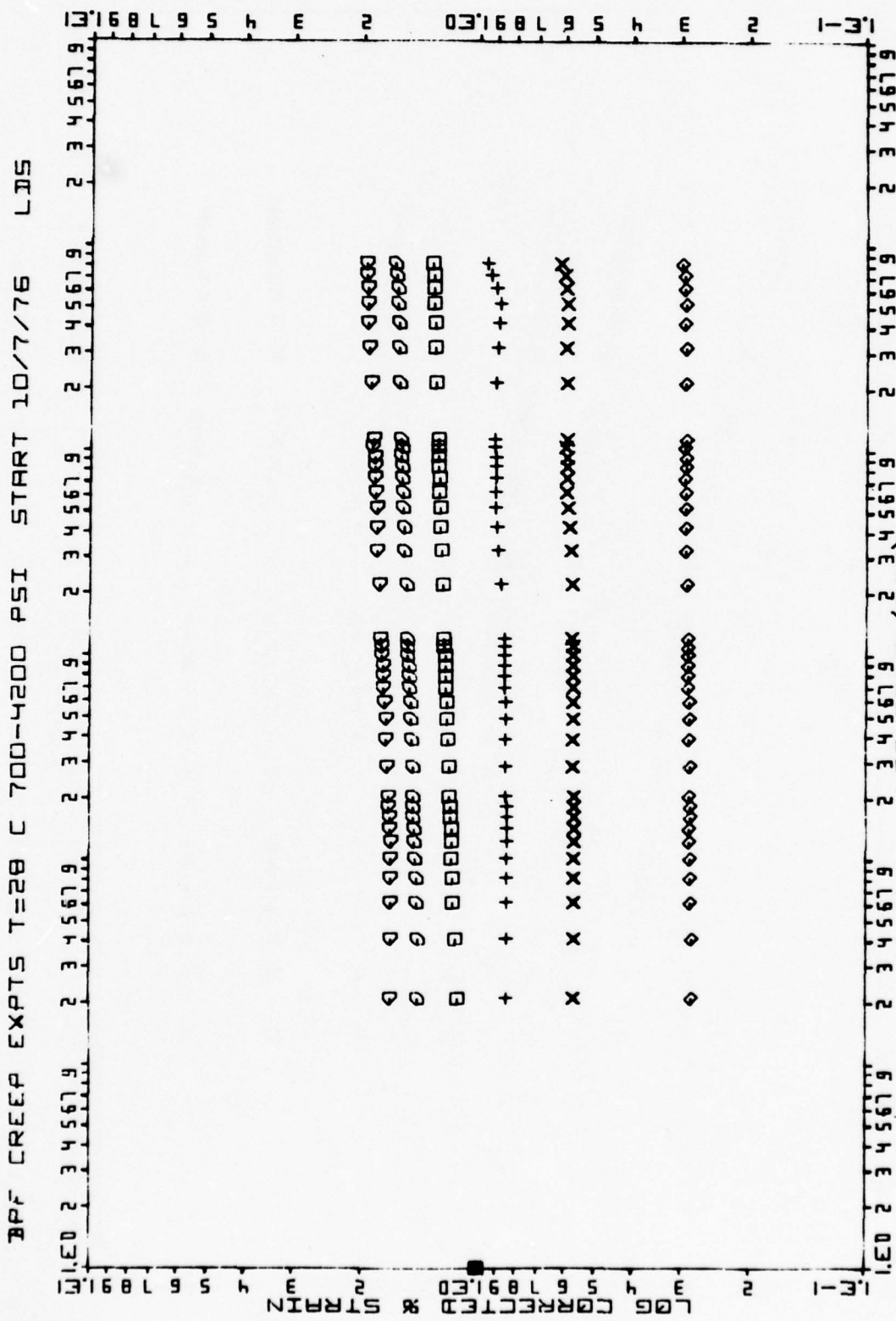

Figure 7. Log creep strain vs log time at 28°C.

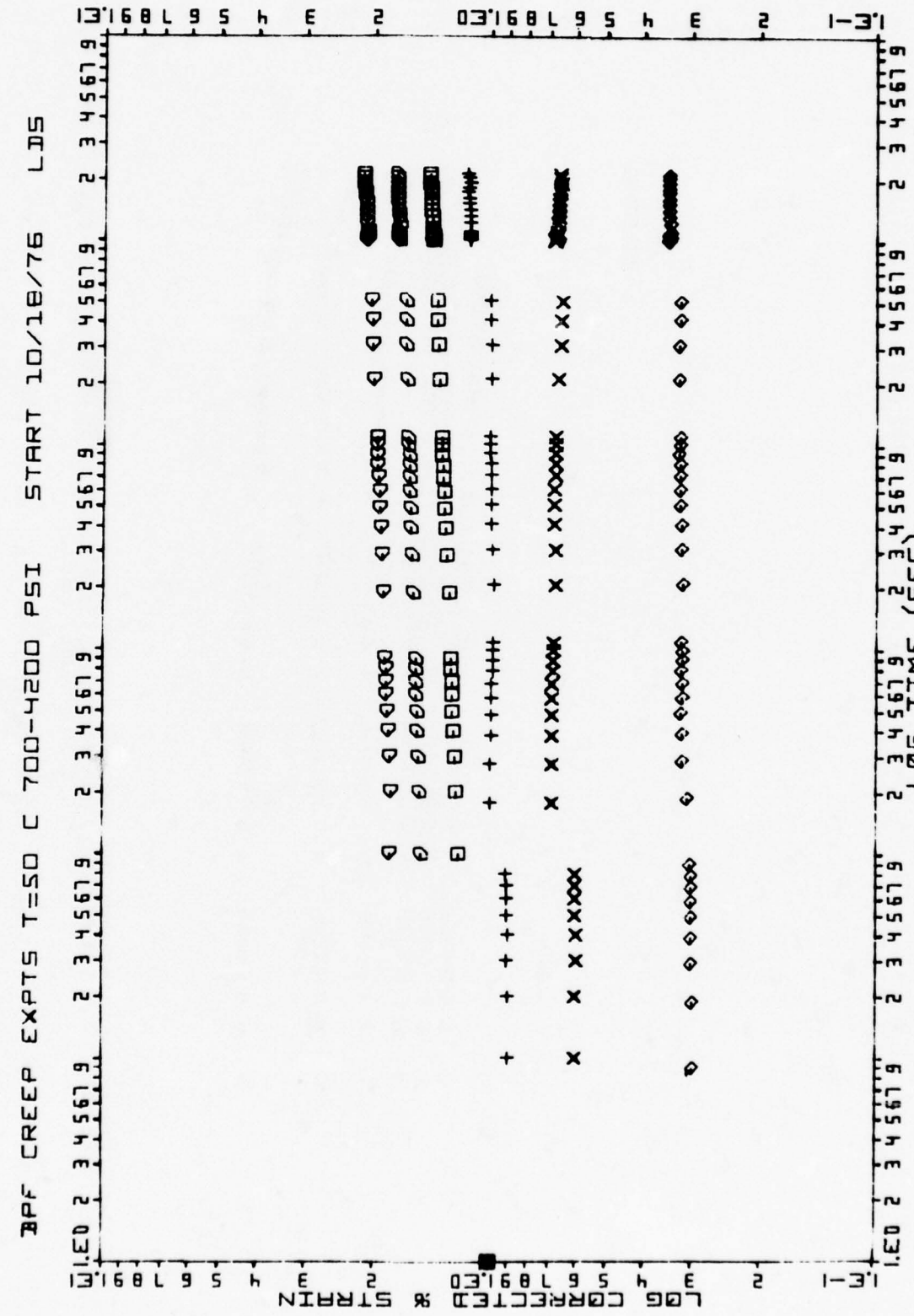

Figure 8. Log creep strain vs log time at 50°C.

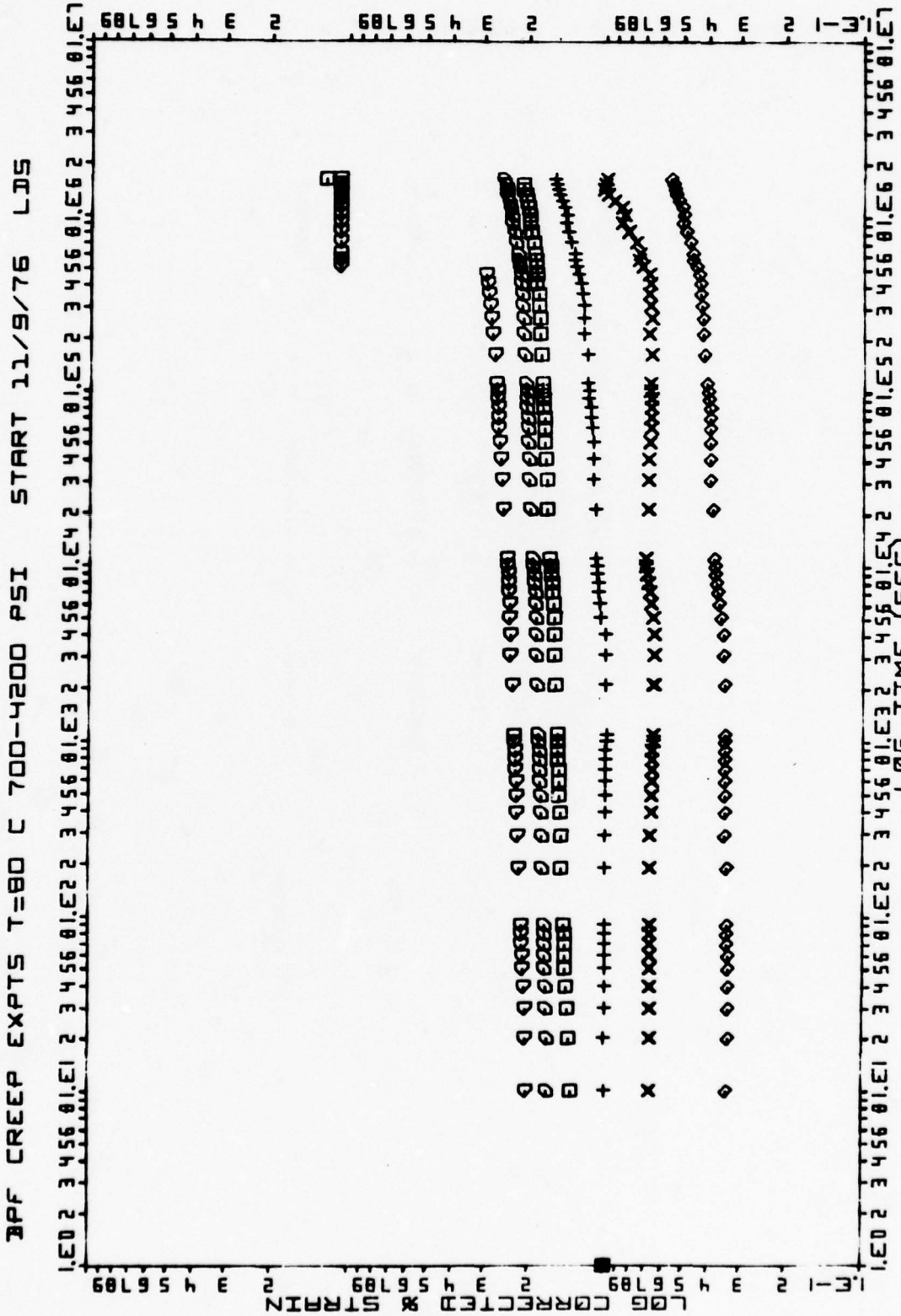

Figure 9. Log creep strain vs log time at 80°C.

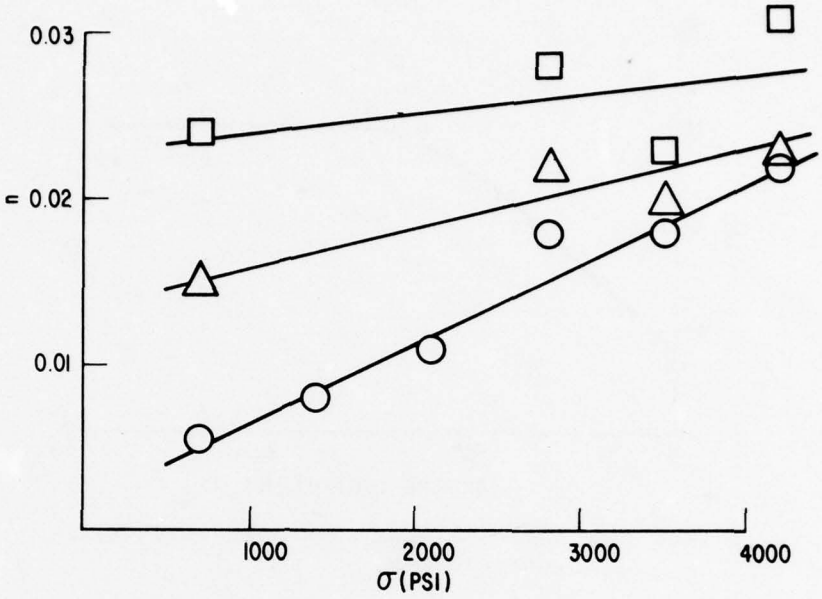

Figure 10. Stress dependence of creep time exponent n: o - 28°C, Δ - 50°C, □ - 80°C.

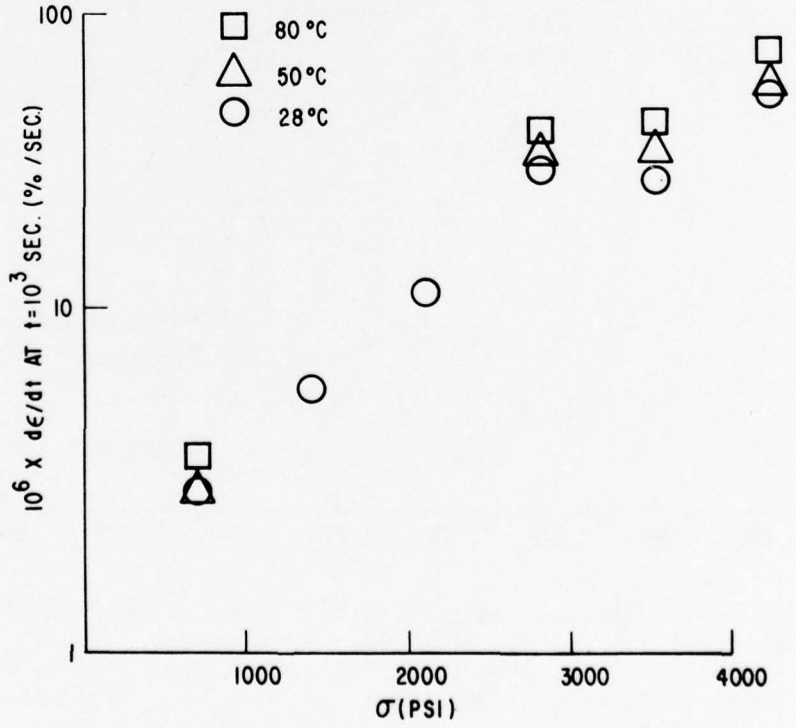

Figure 11. Stress dependence of creep rate at 10^3 seconds: o - 28°C, Δ - 50°C, □ - 80°C.

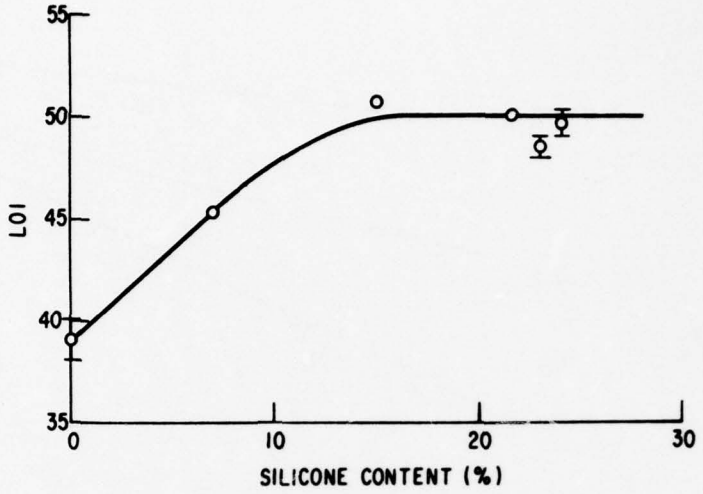

Figure 12. ASTM limiting oxygen index vs silicone content.

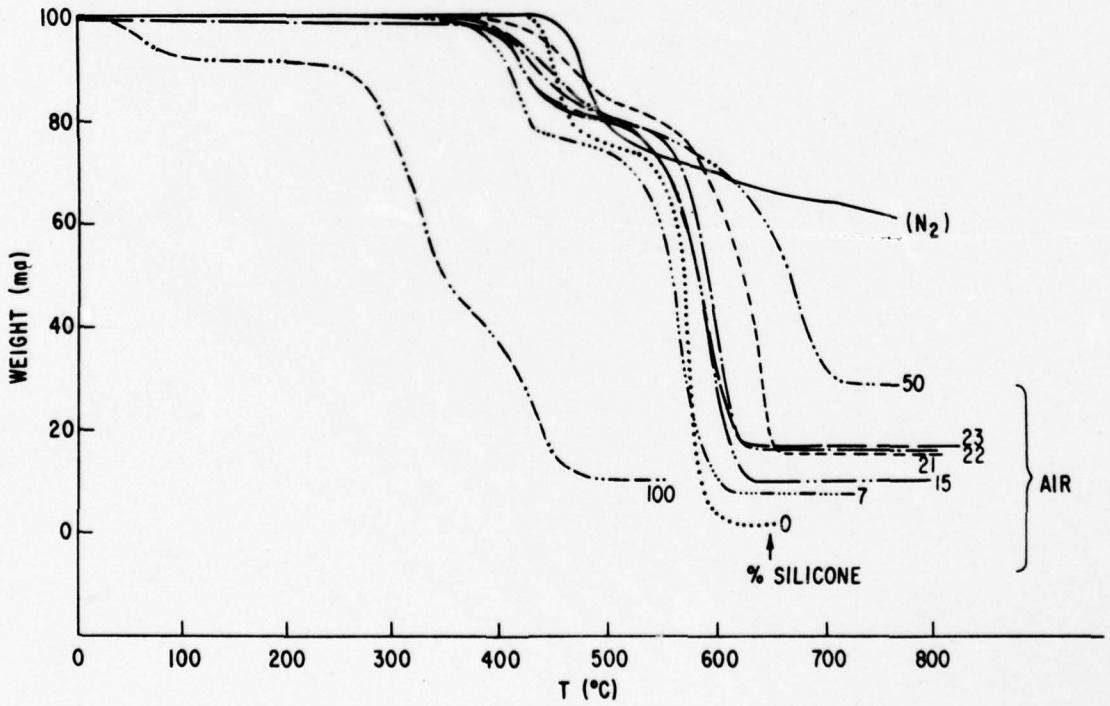

Figure 13. Thermogravimetric analyses of BPF polycarbonate in nitrogen and of silicone gum and all BPFC/DMS resins in air. Code: —— BPF PC in nitrogen; ..... BPF PC; — · — · — · — .10053-129B-3; — — — — 10053-132C; ------ 10053-136C; -..-..-..-.. 10053-151; -....-....-9824-97B-X; ____..____..____ 9824-101A-X; —..—..—..—.. 50 % silicone resin (uncoded); - -..- -.. silicone gum. Numbers on graph indicate silicone weight percentages.

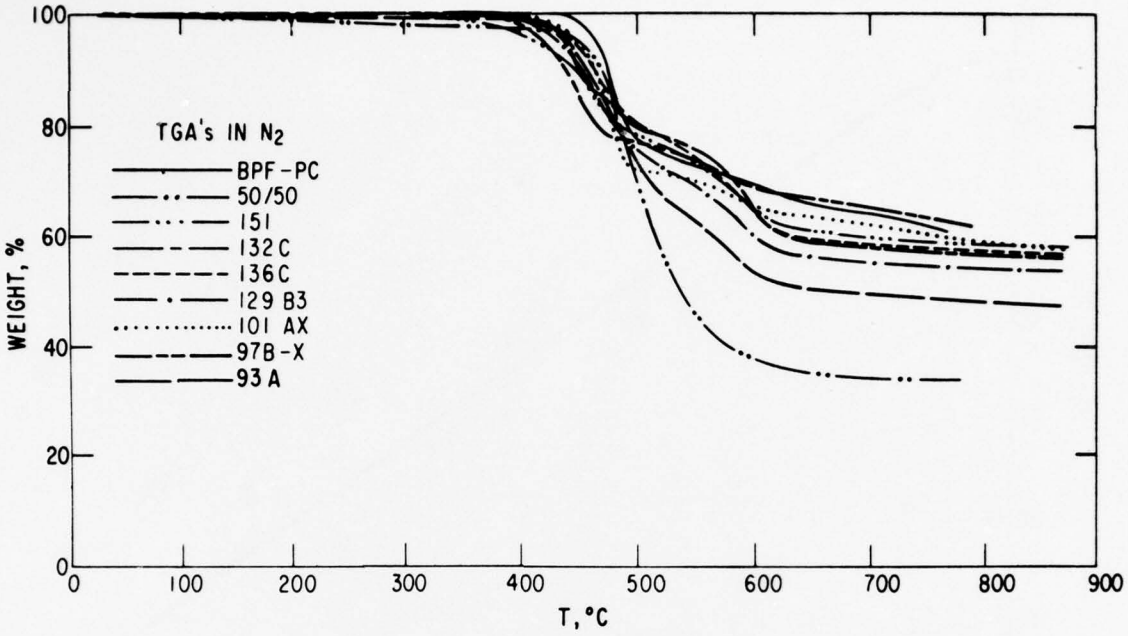

Figure 14. Thermogravimetric analyses of all BPF/DMS resins in nitrogen. Silicone contents given in Figure 13.

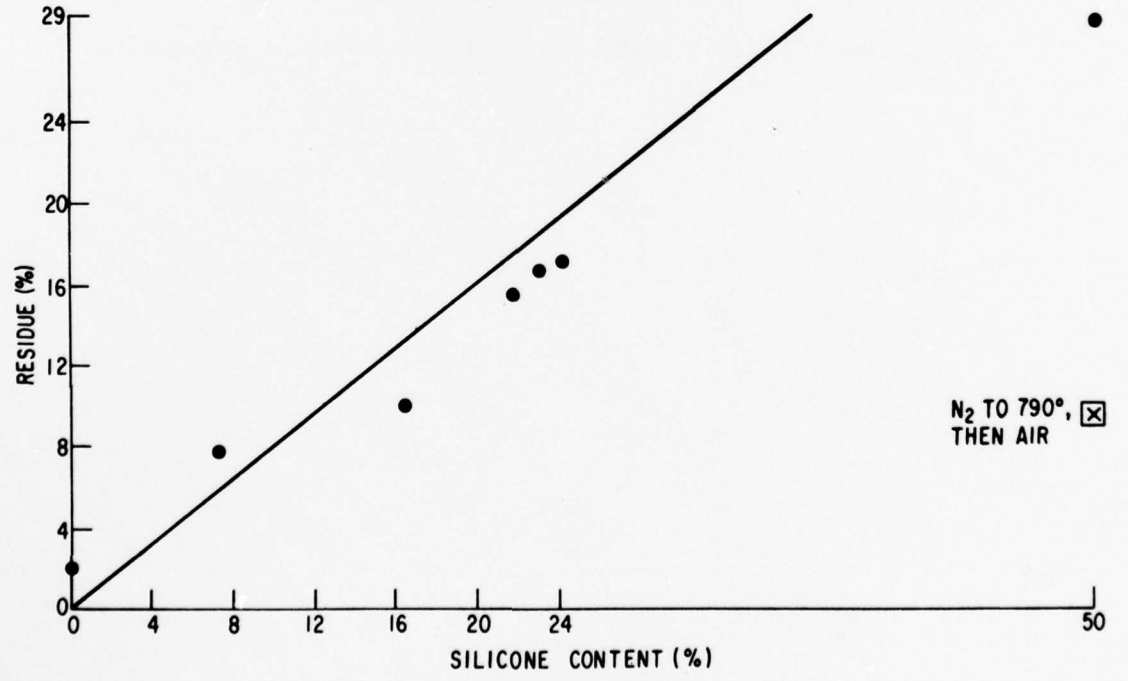

Figure 15. TGA (air) residue at 700°C vs silicone content. Also shown is residue from run in nitrogen to 780°C, followed by air at 700°C until weight loss stopped.

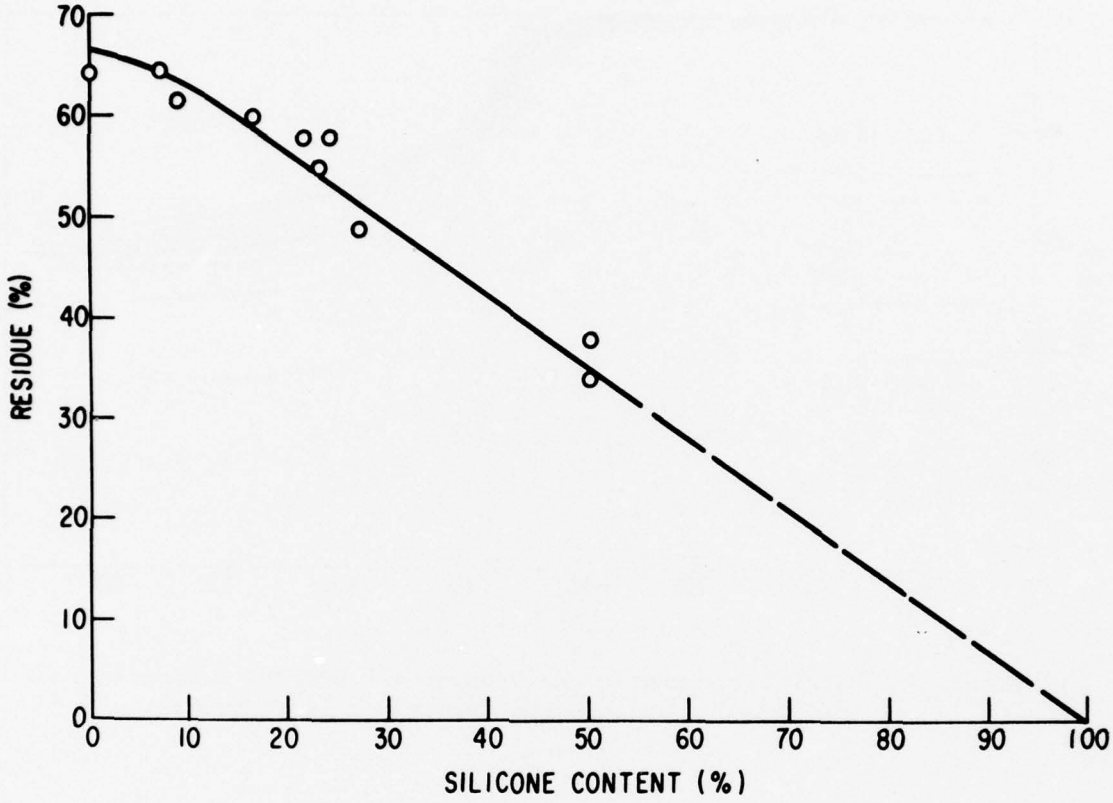

Figure 16. TGA (N_2) residue at 700°C vs silicone content.

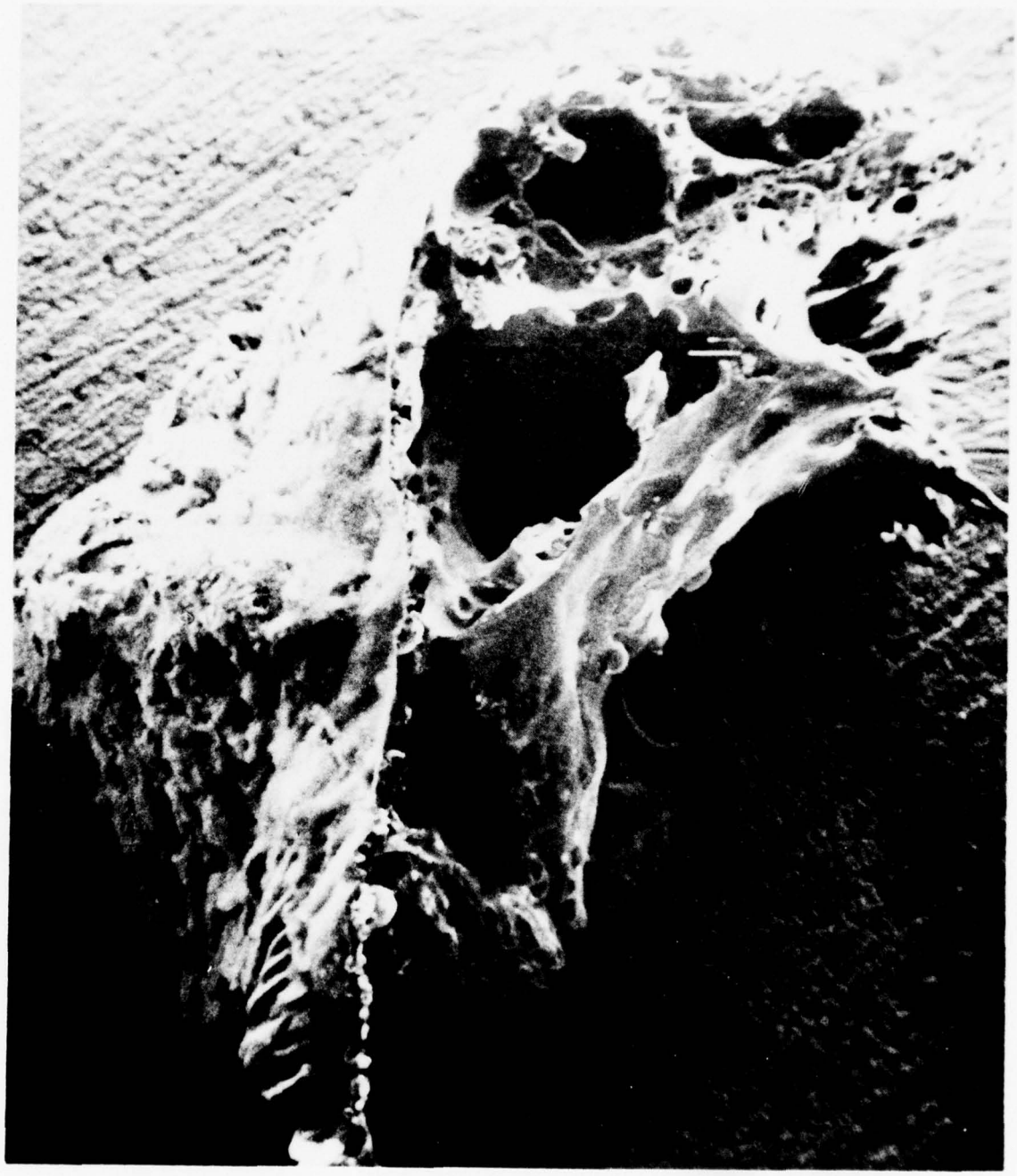

Figure 17. Scanning electron micrograph of LOI char from block polymer 10053-136C (21.5 % silicone) before mounting in epoxy. (Magnification 50X)

Figure 18. Petrographic section of LOI char 10053-136C vacuum-impregnated with epoxy. A few air bubbles still present in epoxy. Thin external char layer is totally black. Internal regions all light-transmitting to varying degrees. Transmitted light.

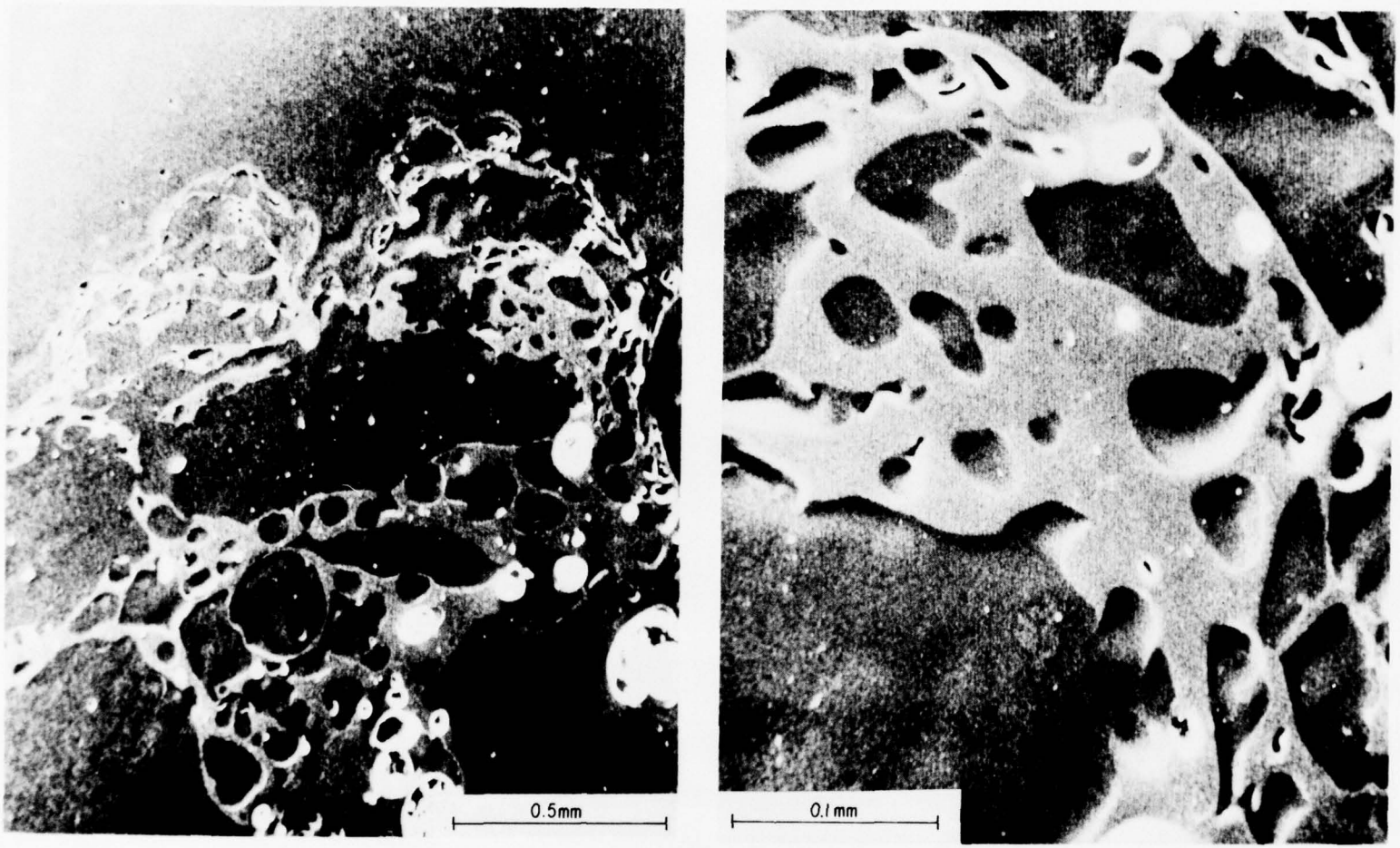

Figure 19. a) Scanning electron micrograph of an external part of char shown in Figures 17 and 18; b) portion of a) at higher magnification.

Figure 20. Scanning electron micrograph formed by using excited silicon X-ray emission intensity of modulate cathode ray tube image. (Same area as in Figure 19b.) Dark regions are epoxy, light regions are char.

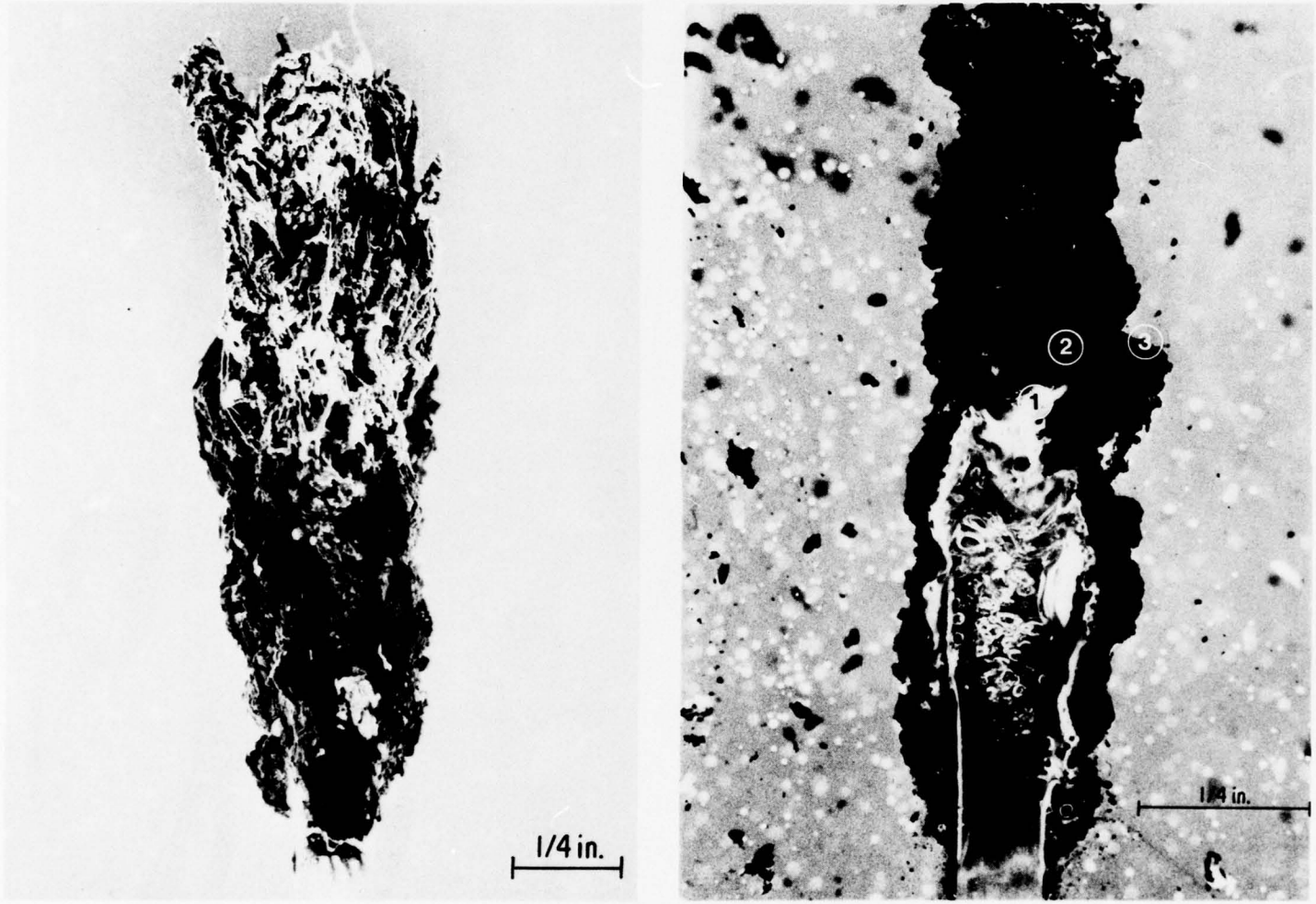

Figure 21. a) Specimen of resin 10053-136C, partially burnt at 50 % oxygen, prior to epoxy impregnation; b) section of same specimen after epoxy vacuum impregnation. Ultramicrotomed sections for electron microscopy taken from areas 1, 2, and 3. (Magnification 7X)

Figure 22. Transmission electron micrograph (TEM) of ultrasection from region 1, Figure 21b. (Magnification 5000X)

Figure 23. TEM of globule in region 1, Figure 21b. (Magnification 25000X)

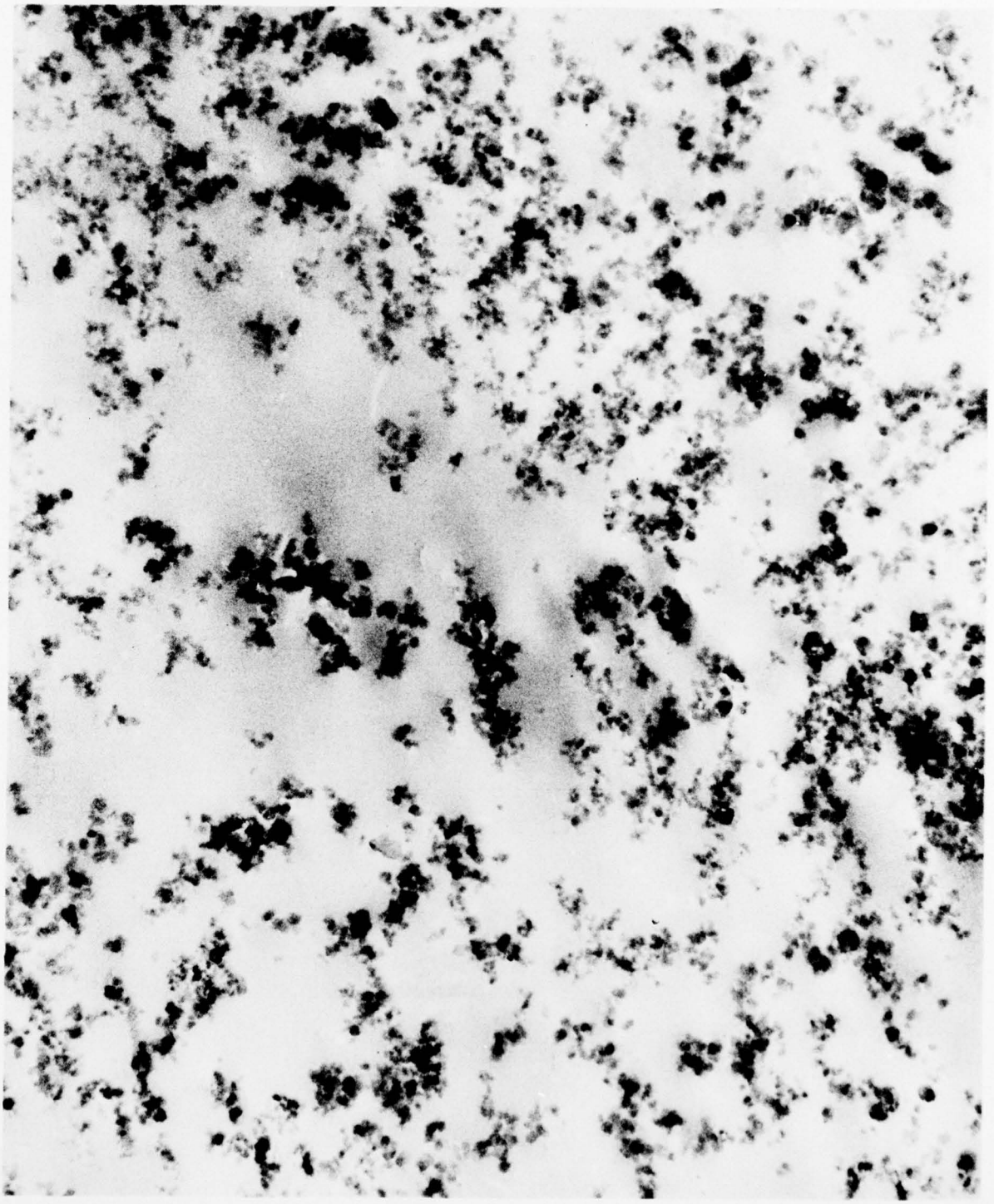

Figure 24. TEM of ultrasection from region 2, Figure 21b. (Magnification 25000X)

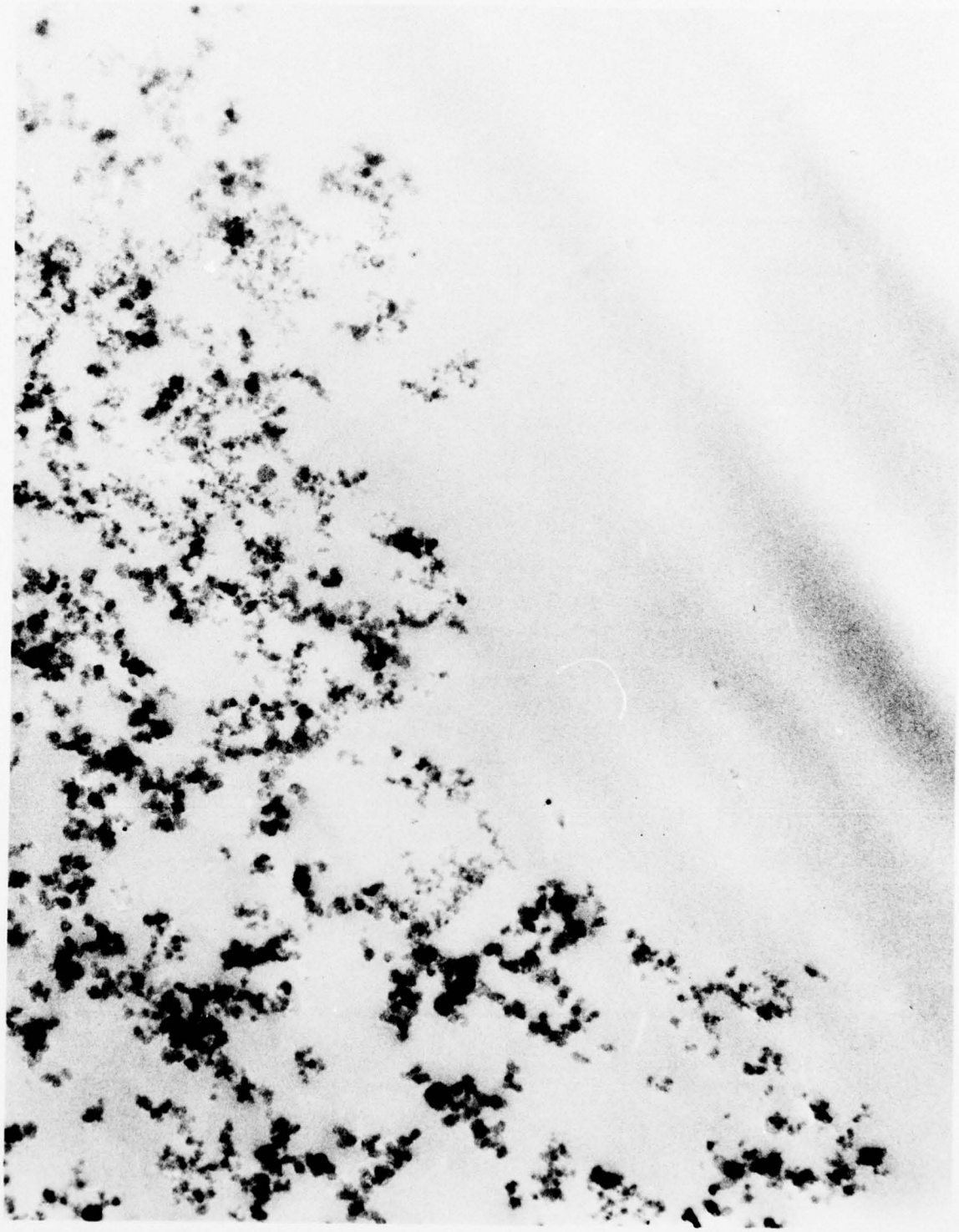

Figure 25. TEM of external edge of char in region 3, Figure 21b. (Magnification 25000X)

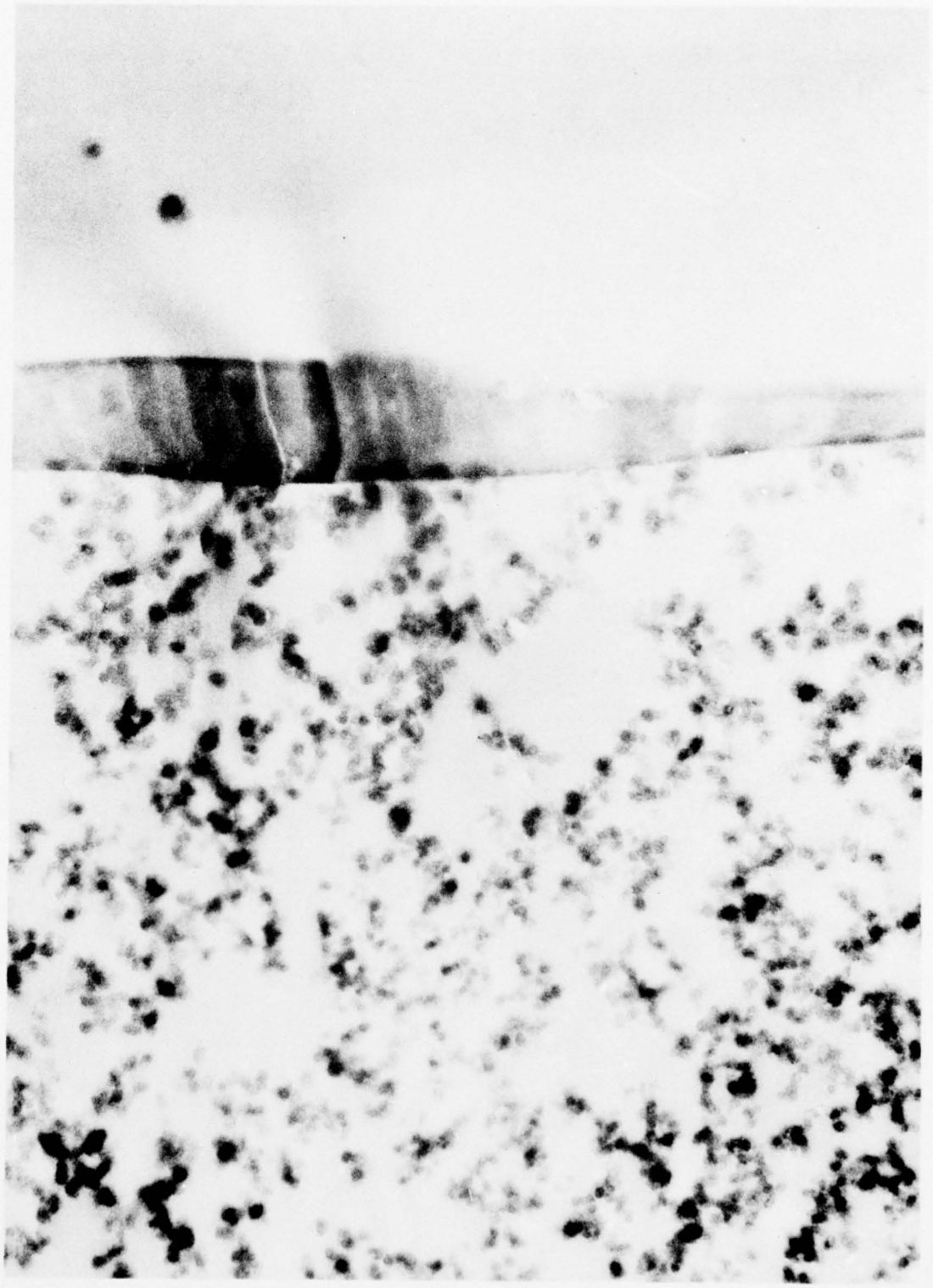

Figure 26. TEM of region 3 showing internal channel with wall lining. (Magnification 25000X)

Figure 27. TEM of region 3 showing internal channel with subdivisions of same material as wall lining. (Magnification 7500X)

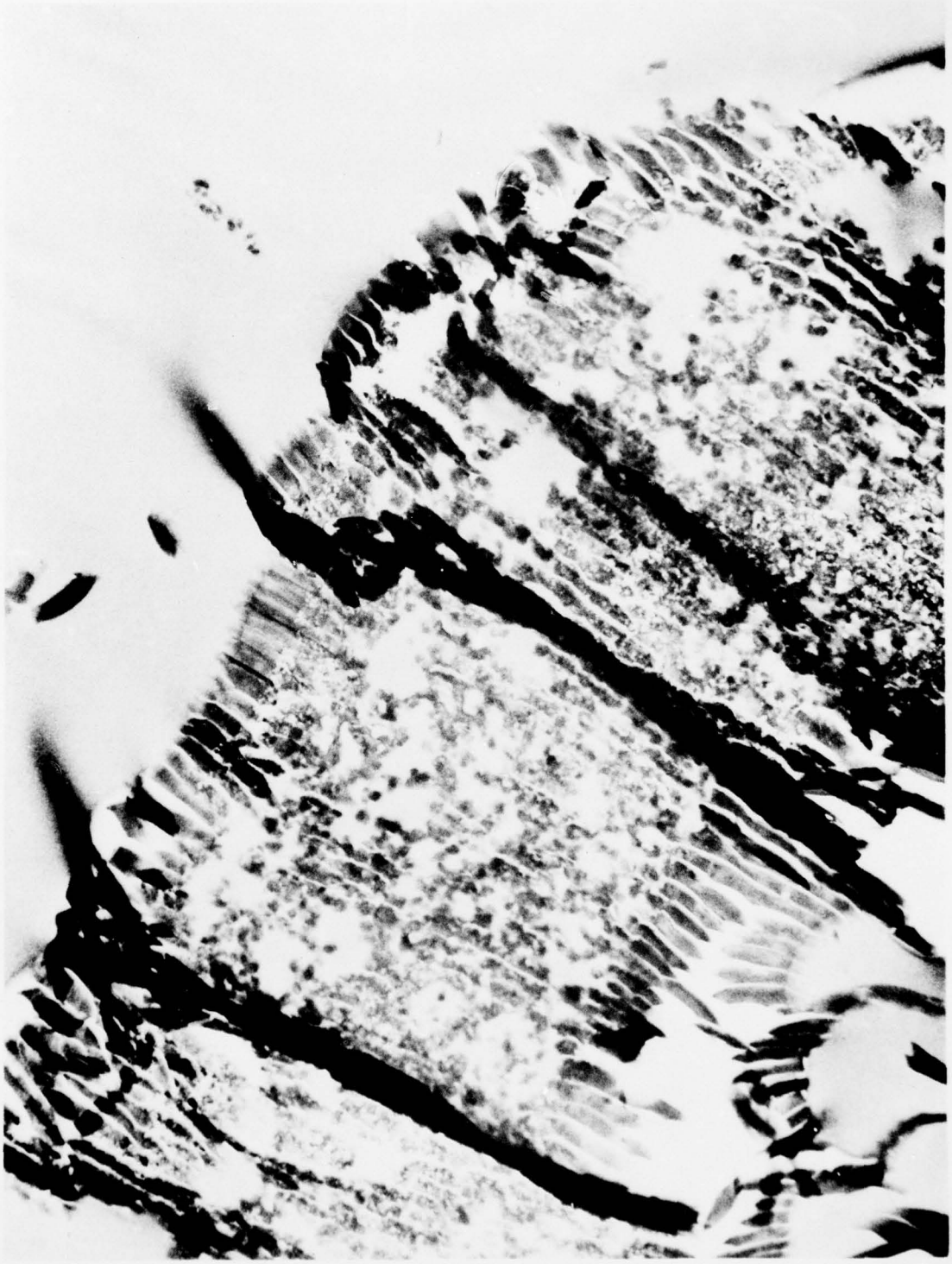

Figure 28. TEM of region 3 showing fractured lining material. (Magnification 7500X)

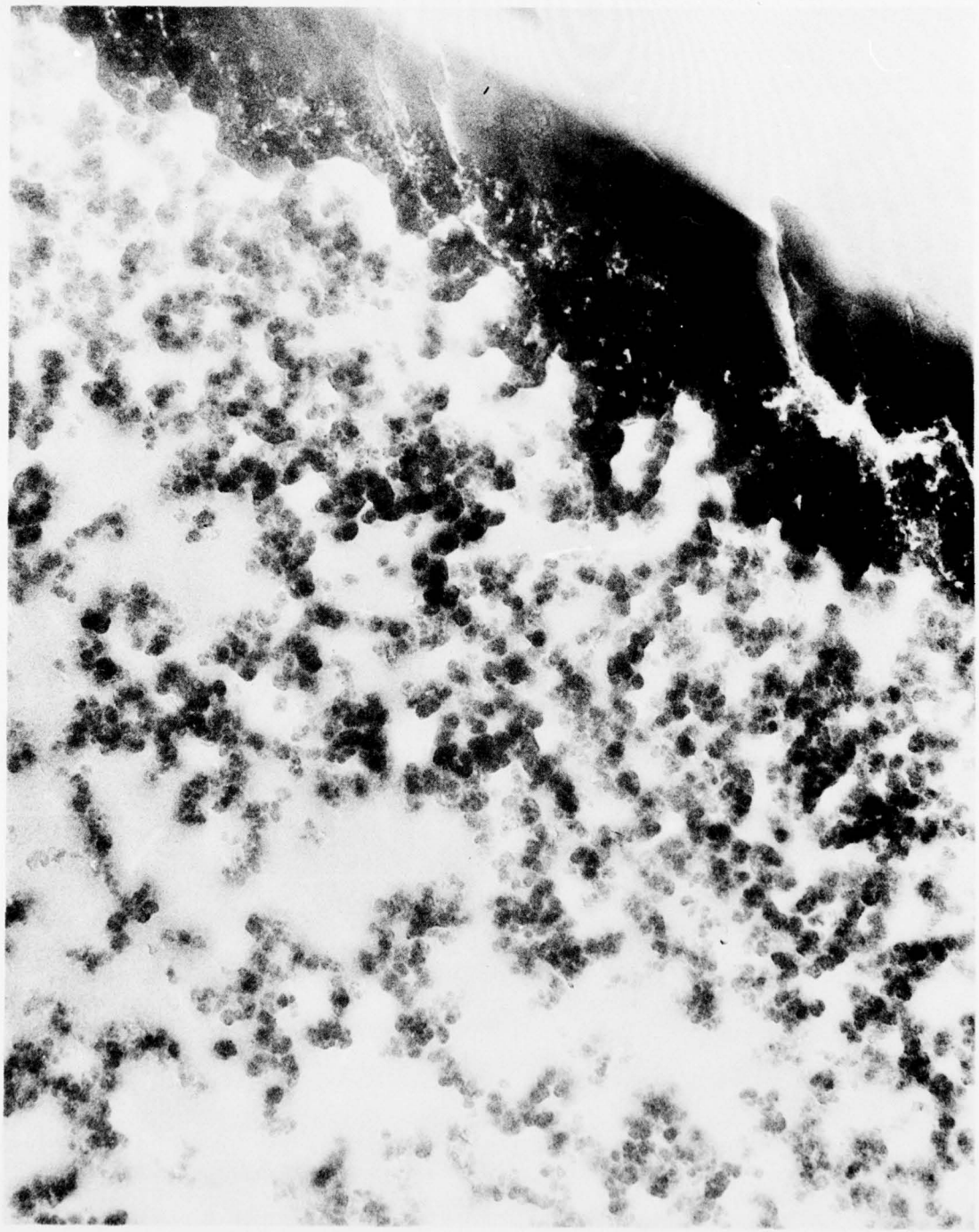

Figure 29a. TEM's of region 3 showing channel lining (upper right) before electron beam intensity was raised to maximum to burn away resinous materials. (Magnification 20000X)

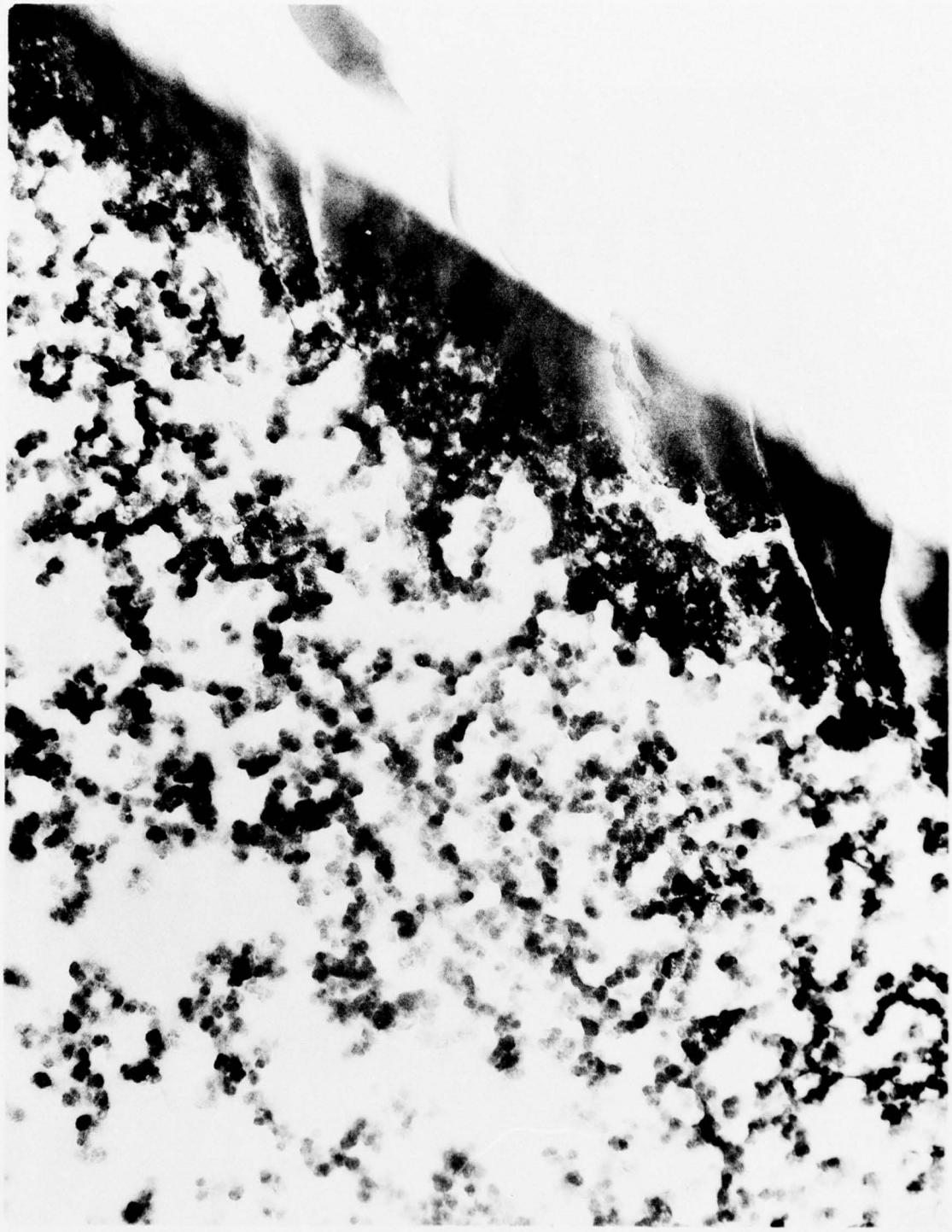

Figure 29b. TEM's of region 3 showing channel lining (upper right) after electron beam intensity was raised to maximum to burn away resinous materials. (Magnification 20000X)

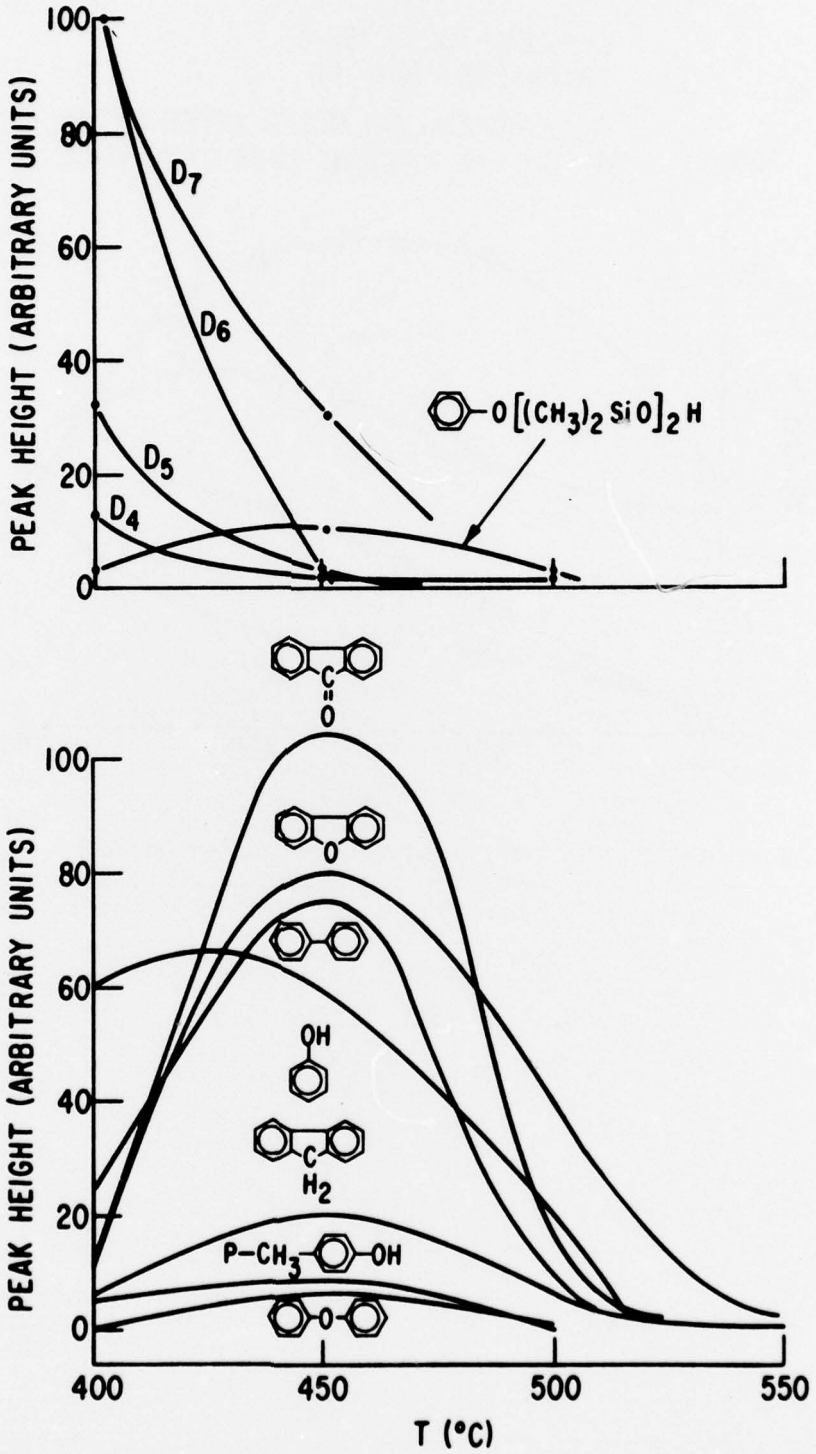

Figure 30. Major volatile products collected in Tenax tubes from thermo-oxidative degradation of one sample of block polymer 10053-132C (24 % silicone) at successively higher temperatures.

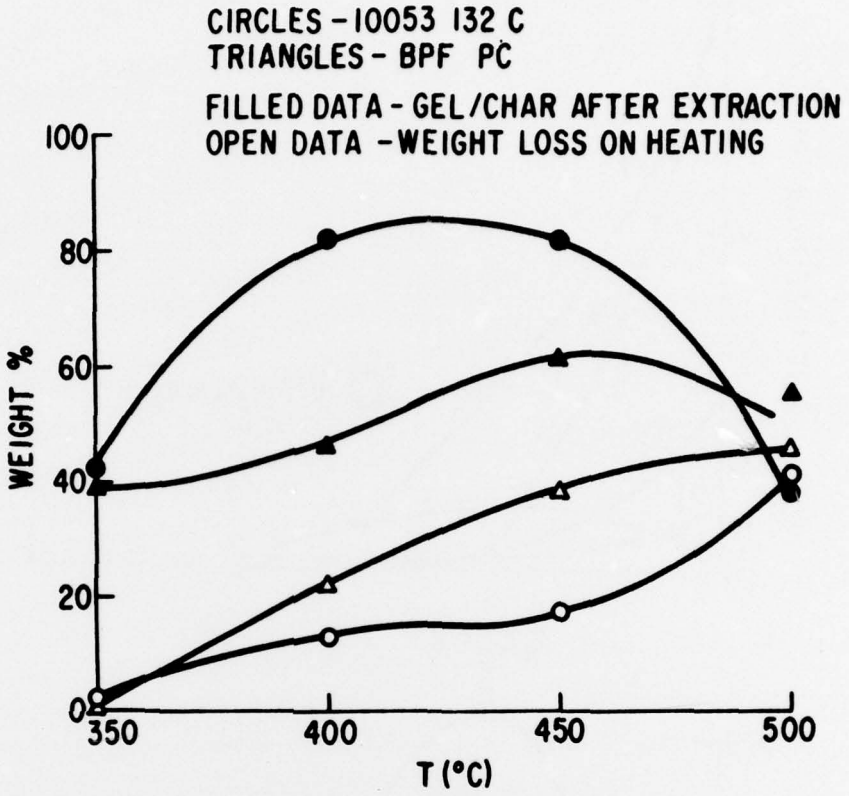

Figure 31. Weight loss and insoluble fraction produced by thermo-oxidative degradation of samples of BPF polycarbonate and block polymer 10053-132C at each of several temperatures.

DISTRIBUTION LIST FOR CONTRACT N00019-76-C-0096
with General Electric Co. Corporate Research and Development

Naval Air Systems Command — 51
Washington, D.C. 20361
Attn: AIR-954 (14 copies)
AIR-530322 (1 copy)
AIR-52032E (36 copies)

Office of Naval Research — 1
Washington, D.C. 20361
Attn: Code 472

Naval Research Laboratory — 2
Washington, D.C. 20375
Attn: Code 8433

Naval Surface Weapons Center — 1
Silver Spring, Maryland
Attn: Code 234

Naval Air Development Center — 1
Warminster, Pennsylvania 18974
Attn: Code 302

Naval Weapons Center — 1
China Lake, California 93555
Attn: Code 5516

Air Force Materials Laboratory — 2
Wright-Patterson AF Base, Ohio 45433
Attn: MXE (S. Marolo, 1 copy)
MBP (H. Rosenberg, 1 copy)

Air Force Flight Dynamics Laboratory — 2
Wright-Patterson AF Base, Ohio 45433
Attn: FEW (R. Wittman)

NASA Headquarters — 1
Washington, D.C. 20546
Attn: B.G. Achhammer

NASA Ames Research Center — 1
Moffitt Field, California 94035
Attn: Dr. John Parker

Materials Sciences Laboratory — 1
Army Materials and Mechanics Research Center
Watertown, Massachusetts 02172
Attn: Dr. Robert Lewis

U.S. Army Aviation Materiel Laboratories — 1
Fort Eustis, Virginia 23604

PLASTEC — 1
Picatinny Arsenal
Dover, New Jersey 07801

Goodyear Aerospace Corporation — 2
Litchfield Park, Arizona 85340
Attn: J. Harman

Swedlow, Inc. — 2
12605 Beach Boulevard
Garden Grove, California 92642
Attn: K. Granger

Sierracin Corporation — 2
12780 San Fernando Road
Sylmar, California 91342
Attn: George Wiser

Texstar Plastics — 1
P.O. Box 1530
Grand Prairie, Texas 75050

Fortin Plastics, Inc. — 1
28687 Golden State Highway
Valencia, California 91355

PPG Industries, Inc. — 2
Box 2200
Huntsville, Alabama 35800
Attn: J.S. Mazza

The Boeing Company — 1
Supersonic Transport Division
Seattle, Washington 98124
Attn: P.N. Beaumont

LTV Aerospace Corporation — 1
P.O. Box 5907
Dallas, Texas 75222
Attn: A. Hohman

Beech Aircraft Corporation — 1
Engineering R&D
9707 E. Central
Wichita, Kansas 67201

Lockheed Georgia Co. — 1
South Cobb Drive
Marietta, Georgia 30060

McDonnell Douglas Corporation 2
McDonnell Aircraft Co.
Box 516
St. Louis, Missouri 63166
Attn: E.R. Fannin (1 copy)
R.A. Lammers III (1 copy)

Lockheed-California Co. 1
Materials Engineering Dept.
Burbank, California 91503

Grumman Aerospace Corporation 1
Bethpage, Long Island, New York 11714
Attn: J.M. Myles

McDonnell Douglas Corporation 3
Douglas Aircraft Co.
3855 Lakewood Blvd.
Long Beach, California 90846
Attn: J.W. Kozmota (1 copy)
O. Minnich (1 copy)
Technical Library, C1 290/36-84 (1 copy)

Rockwell International 2
International Airport
Los Angeles, California 90009
Attn: James Mahaffey (1 copy)
R. Morrow, Dept. 115-062 (1 copy)

Northrop Corporation 1
Airplane Division
3901 W. Broadway
Hawthorne, California 90045

Fairchild Hiller Corporation 1
Republic Aviation Division
Farmingdale, Long Island, New York 11735

Rohm and Haas Company 1
Plastics Department
Independence Mall West
Philadelphia, Pennsylvania 19105
Attn: Orville Pierson

The Rand Corporation 1
1700 Main Street
Santa Monica, California 90406
Attn: Donald F. Adams

Aerospace Corporation 1
Materials Laboratory
2400 East El Segundo Blvd.
El Segundo, California 90245

Aerospace Industrial Association 1
1725 DeSales St. N.W.
Washington, D.C. 20036

Rockwell International 1
Columbus Division
4300 E. Fifth Avenue
Columbus, Ohio 43219
Attn: Gail Clark

Monsanto Research Corporation 1
1101 - 17th Street, N.W.
Washington, D.C. 20036

Union Carbide Corporation 1
Chemicals and Plastics
River Road
Bound Brook, New Jersey 08805
Attn: Dr. W.P. Samuels, Jr.

Hughes Aircraft Company 1
Culver City, California 90230
Attn: S. Schwartz

Bell Helicopter Company 1
P.O. Box 482
Fort Worth, Texas 76101
Attn: Robert Seago